Ion Interactions in the High-affinity Binding Locus of a Voltage-gated Ca^{2+} Channel

Robin K. Cloues, Susan M. Cibulsky, and William A. Sather

From the Department of Pharmacology and Neuroscience Center, University of Colorado Health Sciences Center, Denver, Colorado 80262

ABSTRACT The selectivity filter of voltage-gated Ca^{2+} channels is in part composed of four Glu residues, termed the EEEE locus. Ion selectivity in Ca^{2+} channels is based on interactions between permeant ions and the EEEE locus: in a mixture of ions, all of which can pass through the pore when present alone, those ions that bind weakly are impermeant, those that bind more strongly are permeant, and those that bind more strongly yet act as pore blockers as a consequence of their low rate of unbinding from the EEEE locus. Thus, competition among ion species is a determining feature of selectivity filter function in Ca^{2+} channels. Previous work has shown that Asp and Ala substitutions in the EEEE locus reduce ion selectivity by weakening ion binding affinity. Here we describe for wild-type and EEEE locus mutants an analysis at the single channel level of competition between Cd^{2+}, which binds very tightly within the EEEE locus, and Ba^{2+} or Li^{+}, which bind less tightly and hence exhibit high flux rates: Cd^{2+} binds to the EEEE locus $\sim 10^4\times$ more tightly than does Ba^{2+}, and $\sim 10^8\times$ more tightly than does Li^{+}. For wild-type channels, Cd^{2+} entry into the EEEE locus was 400× faster when Li^{+} rather than Ba^{2+} was the current carrier, reflecting the large difference between Ba^{2+} and Li^{+} in affinity for the EEEE locus. For the substitution mutants, analysis of Cd^{2+} block kinetics shows that their weakened ion binding affinity can result from either a reduction in blocker on rate or an enhancement of blocker off rate. Which of these rate effects underlay weakened binding was not specified by the nature of the mutation (Asp vs. Ala), but was instead determined by the valence and affinity of the current-carrying ion (Ba^{2+} vs. Li^{+}). The dependence of Cd^{2+} block kinetics upon properties of the current-carrying ion can be understood by considering the number of EEEE locus oxygen atoms available to interact with the different ion pairs.

KEY WORDS: selectivity • permeability • site-directed mutagenesis • ion channel

INTRODUCTION

How an ion channel can be highly discriminating in its choice of permeant ion while also supporting very rapid flux of that same ion species is a question that has attracted scrutiny for more than three decades (Hille, 1992). Understanding this achievement by K^{+} and Ca^{2+} channels, which exhibit error rates of only one ion per several thousand transported during a typical 1-ms opening, has been especially interesting because both of these classes of channels are commonly thought to achieve their unusually high degree of selectivity via binding of the preferred ion (Hodgkin and Keynes, 1955; Hille and Schwarz, 1978; Armstrong and Taylor, 1980; Almers and McCleskey, 1984; Hess and Tsien, 1984; Hess et al., 1986; Lansman et al., 1986; Neyton and Miller, 1988a,b; Miller, 1999). It has been known for many years that K^{+} channels are sized to fit bare K^{+} ions (2.66 Å radius) and cannot fit, in an energetic sense, smaller Na^{+} ions (1.90 Å) (Bezanilla and Armstrong, 1972; Hille, 1973). The recently obtained crystal structure of a bacterial K^{+} channel has beautifully confirmed this view (Doyle et al., 1998).

In contrast to most K^{+} channels (but see Armstrong and Miller, 1990; Korn and Ikeda, 1995), Ca^{2+} channels readily transport ions other than Ca^{2+} when the preferred ion, Ca^{2+} (1.98 Å diameter), is removed from the bathing medium. From steric considerations alone, this can occur because the Ca^{2+} channel pore has a relatively wide diameter of 6 Å (McCleskey and Almers, 1985), which allows ions such as Na^{+} to pass through unhindered even in a partly hydrated state. Under physiological conditions of approximately millimolar extracellular Ca^{2+}, Ca^{2+} channels selectively transport Ca^{2+} and not Na^{+} because Ca^{2+} binding within the single-file pore blocks Na^{+} flux. As noted by Bezanilla and Armstrong (1972), pore binding of a preferred permeant ion, though advantageous for selectivity, retards movement of the preferred ion through the pore. Ca^{2+} channels circumvent this problem by allowing interaction between ions within the pore, in such a manner that Na^{+} ions are ineffective at dislodging a bound Ca^{2+} ion (thus block and selectivity), but entry of an-

Address correspondence to William A. Sather, Neuroscience Center, Box B-138, University of Colorado Health Sciences Center, 4200 East Ninth Avenue, Denver, CO 80262. Fax: 303-315-2503; E-mail: william.sather@uchsc.edu

other Ca^{2+} ion increases the exit rate of the bound Ca^{2+} ion 20,000-fold (thus high unitary current) (Almers and McCleskey, 1984; Hess and Tsien, 1984; Tsien et al., 1987; Yue and Marban, 1990). These multi-ion phenomena were originally described using models that incorporated two high-affinity binding sites for Ca^{2+}, but other models have been put forward as well, including models with a single high-affinity site (Armstrong and Neyton, 1991; Dang and McCleskey, 1998) or even no formal binding site (Nonner and Eisenberg, 1998; Nonner et al., 1999). As presently constituted, this latter no-site model is unsuccessful in accounting for some key aspects of the experimentally observed behavior of Ca^{2+} channels, however (McCleskey, 1999).

In its details, the original two-site model also does not provide an accurate description of selective ion transport in Ca^{2+} channels. Most significantly, site-directed mutagenesis work has revealed not two high-affinity Ca^{2+} binding sites, but instead a locus of four pore-lining glutamate (E) residues that collectively can bind a single Ca^{2+} ion with high affinity or multiple Ca^{2+} ions with low affinity (Kim et al., 1993; Mikala et al., 1993; Tang et al., 1993; Yang et al., 1993; Yatani et al., 1994). The effects on Ca^{2+} binding affinity of mutations in the glutamate locus (EEEE locus) have been investigated for Ca^{2+} entering the pore from either side of the membrane, and this work has shown that the EEEE locus is the only high-affinity Ca^{2+} binding structure in the pore of Ca^{2+} channels (Yang et al., 1993; Ellinor et al., 1995; Cibulsky and Sather, 2000). Although each of the four glutamates interacts with Ca^{2+}, they do so with dissimilar strengths of interaction (Mikala et al., 1993; Yang et al., 1993; Ellinor et al., 1995; Parent and Gopalakrishnan, 1995). Thus, the degree to which Ca^{2+} binding was reduced depended upon which glutamate residue was replaced. An attractive rationale for this is that the different glutamates carry out distinct roles in interacting with permeant ions entering and exiting the EEEE locus, with neighboring, nonglutamate residues involved in tuning the affinity of individual EEEE locus residues. The structural origins of this functional asymmetry within the EEEE locus have only been incompletely identified (Williamson and Sather, 1999).

In previous work, the pattern of EEEE locus interactions with mono- and divalent cations also depended upon the chemical nature (aspartate, glutamine, alanine) of the substitutions introduced and upon the specific pair of ions chosen for competition (Ca^{2+} vs. Li^+, Cd^{2+} vs. Li^+, or Cd^{2+} vs. Ba^{2+}) (Ellinor et al., 1995). Here we describe the effects of amino acid substitutions in the EEEE locus upon the kinetics of Cd^{2+} block of unitary divalent (Ba^{2+}) and monovalent (Li^+) currents carried by α_{1C} Ca^{2+} channels. The nature of the interaction between EEEE locus glutamate residues and permeant ions was investigated by analyzing the effects of the mutations upon rates of entry and exit for Cd^{2+}, a pore-blocking ion that binds in the EEEE locus with very high affinity.

Based on the fact that aspartate and alanine substitutions in the EEEE locus reduced binding affinity for Cd^{2+} (Ellinor et al., 1995), one simple expectation for our single-channel block experiments was that Cd^{2+} off rate would increase in the mutants. A second simple expectation was that in mutants with reduced EEEE locus charge (alanine substitutions), Cd^{2+} on rate might also be decreased owing to a weaker electrostatic attraction. Neither of these expectations was fulfilled. Instead, we found that when probed with a monovalent current-carrying ion, EEEE locus substitution mutants exhibited retarded rates of blocker entry, but when probed with a divalent current carrier, these same mutants exhibited enhanced rates of blocker exit. These results can be understood by considering the numbers of EEEE locus oxygen atoms available to interact with blocking and current-carrying ions, as developed in a schematic model presented in the DISCUSSION.

MATERIALS AND METHODS

Expression of α_{1C} Ca^{2+} Channels in Xenopus Oocytes

L-type Ca^{2+} channels (α_{1C}, cardiac splice variant) having a subunit composition of $\alpha_{1C}\beta_{2b}\alpha_2\delta_{1a}$ were heterologously expressed in *Xenopus laevis* oocytes, as described previously (Sather et al., 1993; Ellinor et al., 1995). In a recently proposed systematic nomenclature, this channel is referred to as $\alpha_1$1.2a/β2b/$\alpha_2\delta$1a (Ertel et al., 2000). In brief, Ca^{2+} channel cRNAs were synthesized by in vitro transcription using wild-type or mutant versions of the recombinant plasmids pCARDHE (rabbit α_{1C}, gene bank accession number X15539; constructed by subcloning the α_{1C} insert from pCARD3 into a modified version of the pGEM-3Z vector bearing the 5′- and 3′-untranslated regions of the *Xenopus* β globin gene; Liman et al., 1992; Cibulsky and Sather, 2000), pBH17 (β_{2b}, accession number X64298), and pCA1S ($\alpha_2\delta_{1a}$, the skeletal muscle subunit described by Mikami et al., 1989, derived from pSPCA1, 3′-truncated, and subcloned into pCDNA3). Oocytes were obtained from female donor frogs anesthetized by ~30-min immersion in water containing 0.2% tricaine methanesulfonate. Ovarian tissue was removed via an abdominal incision ~5-mm in length, and individual oocytes were isolated from the ovarian tissue by gentle agitation for 90 min in Ca^{2+}-free OR-2 solution containing (mM): 82.5 NaCl, 2 KCl, 1 $MgCl_2$, 5 HEPES, pH 7.5 with NaOH, containing 2 mg/ml collagenase B (Boehringer). Dissociated oocytes were rinsed in fresh OR-2 and the stage V-VI oocytes were selected by hand. These oocytes were injected with cRNAs encoding α_{1C} (0.3 μg/μl), $\alpha_2\delta_{1a}$ (0.3 μg/μl), and β_{2b} (0.8 μg/μl) subunits in a 1:1:1 molar ratio, and were maintained in an incubator at 18°C in ND-96 solution containing (mM): 96 NaCl, 2 KCl, 1.8 $CaCl_2$, 1 $MgCl_2$, 5 HEPES, pH 7.6, supplemented with 2.5 mM sodium pyruvate, penicillin (100 U/ml; Sigma-Aldrich), and streptomycin (0.1 mg/ml; Sigma-Aldrich). Oocytes were incubated for 4–12 d before electrophysiological recording.

Single-Channel Recording

The vitelline membrane was manually removed from oocytes expressing α_{1C} Ca^{2+} channels immediately before patch-clamp experiments, as previously described (Sather et al., 1993). For recording, oocytes were bathed in a high K^+ solution to fix the

membrane potential at ~0 mV. The solution contained (mM): 100 KCl, 10 ethyleneglycol-*O,O′*-bis(2-aminoethyl)-*N,N,N′,N′*-tetraacetic acid (EGTA), 10 HEPES, pH 7.4 with KOH. Cell-attached patch recordings (Hamill et al., 1981) were obtained using borosilicate glass pipets containing either a 110 Ba^{2+} solution (mM): 110 $BaCl_2$, 10 HEPES, pH 7.4 with tetraethylammonium (TEA)-OH, or a 100 Li^+ solution (mM): 100 LiCl, 10 HEPES, 14 TEA-Cl, pH 7.4 with TEA-OH. For solutions used to study Cd^{2+} block of Li^+ current, the Li^+ solution was pretreated with Chelex® 100 (Bio-Rad Laboratories) to reduce contamination by divalent metal cations. After removal of the Chelex® 100 beads, solutions with the desired final concentrations of Cd^{2+} were produced by diluting a 10-mM stock solution of $CdCl_2$ into the Li^+ solution that was otherwise nominally free of divalent cations. For solutions used to study Ca^{2+} block of Li^+ current, Li^+ solutions were not treated with Chelex® 100 and instead contained 10 mM of the Ca^{2+} buffer *N*-(2-hydroxyethyl) ethylenediamine-*N,N′,N′*-triacetic acid (HEDTA). Li^+ solutions with desired free [Ca^{2+}] were obtained by adding calculated amounts of $CaCl_2$ (10 mM stock solution) to the HEDTA-supplemented Li^+ solution, and the pH was adjusted to 7.4 with TEA-OH. The amount of $CaCl_2$ added was calculated using the Chelator program (Theo J.M. Schoenmakers, University of Nijmegen, Nijmegen, The Netherlands).

Single-channel currents were recorded with an Axopatch 200B amplifier (Axon Instruments, Inc.). For all recordings, except those of Ba^{2+} currents carried by the $E_{III}D$ mutant, records were low-pass filtered at 2 kHz (−3 dB) with an eight-pole Bessel filter (Frequency Devices, Inc.) and sampled at 10 kHz using Pulse software (HEKA, distributed by Instrutech Corp.). For Ba^{2+} currents carried by the $E_{III}D$ mutant, data were filtered at 5 kHz, sampled at 25 kHz, and digitally refiltered at 5 kHz. To promote long-lasting channel openings, all experiments were carried out in the presence of 2 μM FPL 64176 (included in the bath solution; RBI). Experiments were carried out at 21–23°C.

Data Analysis

Kinetic analysis of block was carried out using TAC software (Bruxton Corp.) and a 50% threshold criterion. Dwell-time histograms for open and shut states were constructed from idealized records, binned logarithmically (20 bins/decade), and plotted against a square root transformation of the ordinate (number of events/bin). Exponential functions were fit to dwell-time histograms using a maximum likelihood method, and the number of exponential components fit (usually one) was determined using a log likelihood ratio test (Colquhoun and Hawkes, 1995). In this display format, peaks in the fitted function correspond to the time constants of the exponential components (Sigworth and Sine, 1987). The rise time of our recording system (0.166 ms at 2 kHz filtering) limited resolution of kinetic events to those lasting >0.166 ms in all recordings except for Ba^{2+} currents carried by $E_{III}D$ (>0.1 ms); shorter duration events were excluded from the analysis. Artifactual lengthening of the observed open time as a result of missed brief closures was corrected according to the equation $\tau_O = \tau_{O,obs}\exp(-T_d/\tau_C)$, where τ_O is the corrected open-state lifetime, $\tau_{O,obs}$ is the open-state lifetime obtained from histogram fitting, T_d is the system dead time (0.09 ms), and τ_C is the lifetime of the shortest fitted component in the closed-state histogram (Colquhoun and Hawkes, 1995). The complimentary problem of missed brief openings artificially lengthening the measured shut lifetime (τ_S) was minimized by the use of FPL 64176.

Kuo and Hess (1993a) have previously analyzed the error in estimating τ_O and τ_S for Ca^{2+} channels when the effects of missed events are dealt with using the simple correction described above. In their work on divalent cation block of current carried by single L-type Ca^{2+} channels, the same type of experiment carried out here, simulated single channel currents were filtered, digitally sampled and analyzed as for real data, and the measured τ_O and τ_S values obtained in this way were compared with the values of τ_O and τ_S that were used to generate the simulated currents. Following this procedure, errors in estimating k_{on} and k_{off} were found to be in the range of 10–30% when using the missed events correction method that we have used (Kuo and Hess, 1993a).

Owing to the action of FPL 64176, open times in the absence of blocker were often tens of milliseconds in duration (see control records in Fig. 1, A and B, below). Channel closures in the absence of blocker were also generally of long duration, typically >10 ms. Inclusion of blocker (Cd^{2+} or Ca^{2+}) in the pipet solution produced brief interruptions (shut times <1 ms) of the FPL 64176–dependent long-duration openings. Shut times longer than 3.0 ms were excluded from the analysis because these mostly represented closures between channel openings rather than block events. Under these conditions, both the open- and the shut-time histograms were in almost all cases well-fit by single exponential functions, with the single component of the shut time largely representing the blocked time, as described below.

The results were analyzed using a simple kinetic scheme (Scheme I) that incorporates gating transitions (k_{-C}, k_C) between closed (C) and open (O) states, and block ($k_{on} \cdot [X^{2+}]$) and unblock (k_{off}) transitions between open and blocked (B) states (Lansman et al., 1986).

$$C \underset{k_C}{\overset{k_{-C}}{\rightleftharpoons}} O \underset{k_{off}}{\overset{k_{on}[X^{2+}]}{\rightleftharpoons}} B \qquad \text{(SCHEME I)}$$

The values of k_{on} and k_{off} for divalent cation block were determined from measurements of channel open and shut times over a range of blocking ion concentrations ([X^{2+}]). The block and unblock rates were related to the open and shut time constants (τ_O, τ_S) by the following equations: $k_{on} \cdot [X^{2+}] + k_C = 1/\tau_O$ and $k_{off} + k_{-C} = 1/\tau_S$.

The block rate, k_{on}, was obtained as the slope of a linear regression fit to plots of τ_O^{-1} versus [Cd^{2+}], and the [Cd^{2+}]-independent closing rate (k_C; given by the fit intercept on the ordinate) consequently did not significantly distort estimation of k_{on}. Furthermore, in the absence of a blocking ion, pure closing rates (k_C) were obtained and compared with τ_O^{-1} values when blocker was included in the pipet. Closing rates for wild-type and mutant channels ranged from 26 to 323 s^{-1} for Ba^{2+} currents, and from 122 to 357 s^{-1} for Li^+ currents. When a blocking ion, such as Cd^{2+}, was included in the pipet solution, a combination of channel closing and block transitions were recorded, and the frequency of these combined events is referred to here as the shutting rate. The closing rates listed in Table I can be compared with shutting rates that ranged from hundreds to thousands per second, depending upon the concentration of blocker used (see Figs. 2–7). Estimates of k_C obtained from the intercept of the fit with the ordinate ([X^{2+}] = 0) were comparable with values of k_C obtained in the absence of blocker. Overall, estimated rates of block were little affected by contamination with channel closing events.

The unblock rate (k_{off}) and the opening rate (k_{-C}) were both concentration-independent, however, making unambiguous determination of k_{off} more difficult in principle. Nonetheless, accurate estimation of k_{off} was possible because with increasing [X^{2+}] the number of unblock events increased relative to the [X^{2+}]-independent number of opening events. Thus, at higher [X^{2+}], τ_S^{-1} largely reflects k_{off}. How well τ_S^{-1} approximated k_{off} can be appreciated by comparing τ_S^{-1} values measured over a range of [X^{2+}]

TABLE I

Unitary Slope Conductances and Mean Closing and Opening Rates (0 Blocker) for WT, E→D, and E→A Channels

	Ba^{2+}			Li^+		
	g	k_C	k_{-C}	g	k_C	k_{-C}
	pS	s^{-1}	s^{-1}	*pS*	s^{-1}	s^{-1}
WT	33	63 ± 19	3230 ± 310	33	357 ± 125	2630 ± 140
E_ID	20	43 ± 4	4762 ± 1160	14	270 ± 47	2330 ± 270
E_{II}D	16	87 ± 20	4000 ± 320	36	161 ± 4	2440 ± 300
E_{III}D	18	323 ± 52*	11100 ± 1230	45	122 ± 15	2860 ± 80
E_{IV}D	19	73 ± 2	5000 ± 500	30	182 ± 33	5260 ± 139
E_IA	24	96 ± 23	3448 ± 360	29	213 ± 44	5260 ± 1385
E_{II}A	45	26 ± 2	2941 ± 520	31	149 ± 27	5260 ± 554
E_{III}A	15	—	—	36	147 ± 4	6670 ± 890
E_{IV}A	21	107 ± 20	3226 ± 420	40	200 ± 48	4350 ± 1320

Unitary slope conductances were determined from linear regressions fit to data between 0 and −80 mV for Ba^{2+}, and between −40 and −100 mV for Li^+. Listed slope conductances refer only to the largest conductance state observed. Means are reported ± SEM. For Ba^{2+} currents, n = 3–4 patches, except for E_{II}A, where n = 2 patches. For Li^+ currents, n = 3–5 patches, except for E_{IV}A, where n = 2 patches. The mean closing rate (k_C) is $1/\tau_{open}$ and the mean opening rate (k_{-C}) is $1/\tau_{closed}$. Because there were generally several channels in each patch, opening rates represented the composite opening rate for all the n channels present in a patch and, as such, these rates were n-fold greater than the opening rate for a single channel. Gating kinetics were analyzed as for block kinetics (see MATERIALS AND METHODS). *E_{III}D Ba^{2+} data were sampled at 25 kHz and filtered at 3.33 kHz.

(see Figs. 2–7): τ_S^{-1} values did not differ as greatly over a range of $[X^{2+}]$ for a given channel construct (wild type or mutant) as they differed between channel constructs. As a quantitative test, we used simulations to estimate the extent to which potential differences in construct gating might contaminate our estimates of channel block kinetics. We used the simple kinetic scheme described above and computer simulations of worst-case scenarios (SIMU, QuB software suite, available online at http://www.qub.buffalo.edu). In one salient example, the very brief duration of Cd^{2+} block events for E_{III}D Ba^{2+} currents necessitated use of higher sampling and filtering frequencies, which had the consequence of increasing the density of resolved gating events as well (Table I). We therefore simulated an extreme case wherein E_{III}D channels were assumed to be identical to WT in block/unblock kinetics, and differed from WT in gating kinetics alone. The simulated data were analyzed in a manner identical to that used for experimental data. The simulations showed that, when a blocker was present, fast gating in E_{III}D cannot account for the experimentally determined differences between E_{III}D and WT in open- or shut-time constants. Overall, the simulations indicated that construct-dependent differences in gating kinetics of the magnitude observed here do not significantly interfere with estimation of k_{on} and k_{off} for a blocking ion. This was not unexpected, given that the number of unblock events was much greater than the number of opening events over much of the blocker concentration range employed. A similar conclusion was reached in a previous study of L-type Ca^{2+} channels, in which it was found that differences in gating kinetics between subconductance states introduced little error into estimates of Ca^{2+} block kinetics (Cloues and Sather, 2000).

In cases where block kinetics were close to the resolution limit of our recording system, we supplemented the half-amplitude threshold analysis described above with a β-distribution analysis, for which we assumed a reversible two-state block model with transition rates of k_{on} · [blocker] and k_{off} (Yellen, 1984; Pietrobon et al., 1989; Moss and Moczydlowski, 1996). Flickery data that had originally been filtered at 2 or 5 kHz were typically refiltered at 250 Hz using a digital Gaussian filter. The refiltered current amplitudes were normalized ($0 \le i \le 1$) by the open channel amplitude, which was measured for each patch as the difference between well-resolved open and closed levels. To account for instrumentation and other noise unrelated to block and unblock events, a Gaussian function fit to the closed-channel noise was convolved with the normalized β distribution, and the resulting noise-broadened convolution was then fit to the normalized distribution of current amplitudes. The normalized β distribution had the form $f(i) = [i^{a-1} \cdot (1 - i)^{b-1}]/B(a,b)$, where the β function:

$$B(a, b) = \int_0^1 f(i) \cdot di,$$

was used to normalize the distribution, $a = k_{off} \cdot \tau$, $b = k_{on} \cdot [\text{blocker}] \cdot \tau$, $\tau = 0.228/f_c$, and f_c was the calculated −3-dB frequency for the cascaded filters. The β distribution analysis was carried out using a custom-written MATLAB routine (The MathWorks). β distribution analysis was useful for data obtained at higher blocker concentration, where k_{on} and k_{off} were such that $2 \lesssim a,b \lesssim 20$. This method of analysis was tested with simulated data of known kinetics (SIMU), and the rates extracted via the analysis were within 13% of the true rates. In most cases, rates obtained from β distribution analysis of experimental data were within 15% of values obtained from half-amplitude threshold analysis. β distribution analysis was, however, employed solely as an independent methodological test of the fidelity of the half-amplitude threshold analysis.

Nomenclature for Channel Constructs

In the single letter code, glutamate = E, alanine = A, and aspartate = D. The previously identified four glutamate residues that are essential for normal ion selectivity in wild-type Ca^{2+} channels are referred to, in ensemble, as the EEEE locus. Individually, they are designated E_I (E393), E_{II} (E736), E_{III} (E1145), and E_{IV} (E1446), with the Roman numeral subscripts indicating the motif of origin of each glutamate residue. For brevity, mutant channels are symbolized, for example, as E_IA for the E→A substitution in motif I.

All error bars represent SEM, and all mean values are reported together with their standard errors. Student's t test was used to determine statistical significance.

RESULTS

Effect of the Permeant Ion Species on Entry and Exit Rates of a Pore Blocker: Cd^{2+}

Under physiological conditions, Ca^{2+} channels selectively transport Ca^{2+} and not other common cations because Ca^{2+} binding within the channel's pore blocks their flux. We have exploited this basic phenomenon of block to study, at the unitary current level, interactions between permeant cations within the EEEE locus. For wild-type (WT)[1] and mutant α_{1C} Ca^{2+} channels, we measured the kinetics of Cd^{2+} block (on rate, k_{on}) and unblock (off rate, k_{off}) of unitary currents carried by either a divalent cation (Ba^{2+}) or a monovalent cation

[1]*Abbreviation used in this paper:* WT, wild type.

(Li^+). Because α_{1C} Ca^{2+} channels exhibited multiple conductance levels that differ in their on and off rates for blocking ions (Cloues and Sather, 2000), we restricted our analyses of WT and mutant α_{1C} channels to their largest conductance level (Table I). Owing to ion-dependent differences in reversal potential and channel gating, the kinetics of Cd^{2+} block of Ba^{2+} and Li^+ unitary currents could not be resolved at the same voltage, and so current records were collected at 0 mV for Ba^{2+} and at −100 mV for Li^+.

Fig. 1 shows examples of single-channel records carried through WT channels by Ba^{2+} (A) or Li^+ (B). With 0 Cd^{2+} in the patch pipet solution, openings were often tens of milliseconds in duration. When Cd^{2+} was included in the Ba^{2+} or Li^+ pipet solutions, discrete block events were detected as brief interruptions of current flow, and the number of block events increased with [Cd^{2+}]. Half-amplitude threshold analysis of open and shut (blocked) time durations yielded rate constants for pore entry and exit by Cd^{2+}. Shutting rates increased linearly with blocker concentration, in accord with the state diagram described in the MATERIALS AND METHODS.

Entry of Cd^{2+} into the pore was much slower when Ba^{2+}, as compared with Li^+, was the current-carrying ion (Fig. 2, left). The on rate for Cd^{2+} block of Ba^{2+} current was 1.8×10^7 M^{-1} s^{-1} (0 mV), whereas the on rate for Cd^{2+} block of Li^+ current was 8.2×10^9 M^{-1} s^{-1} (−100 mV), an ∼400-fold difference in k_{on} (Table II). On rates for pore blocking ions such as Cd^{2+} are essentially voltage insensitive (Lansman et al., 1986; Kuo and Hess, 1993a,b), as confirmed here by the fact that k_{on} values for Cd^{2+} versus Ba^{2+} were of similar magnitude at 0 mV (1.8×10^7 M^{-1} s^{-1}) and −60 mV (1.1×10^7 M^{-1} s^{-1}; data not shown). In comparing the Ba^{2+} and Li^+ solutions, membrane surface potentials also do not greatly differ (Kuo and Hess, 1992). Thus, the large difference in Cd^{2+} on rate between Ba^{2+} and Li^+ solutions is apparently attributable to differing interactions within the pore between Cd^{2+} and Ba^{2+} in one case, and between Cd^{2+} and Li^+ in the second case.

Rates of Cd^{2+} exit from the pore and into the cytosol

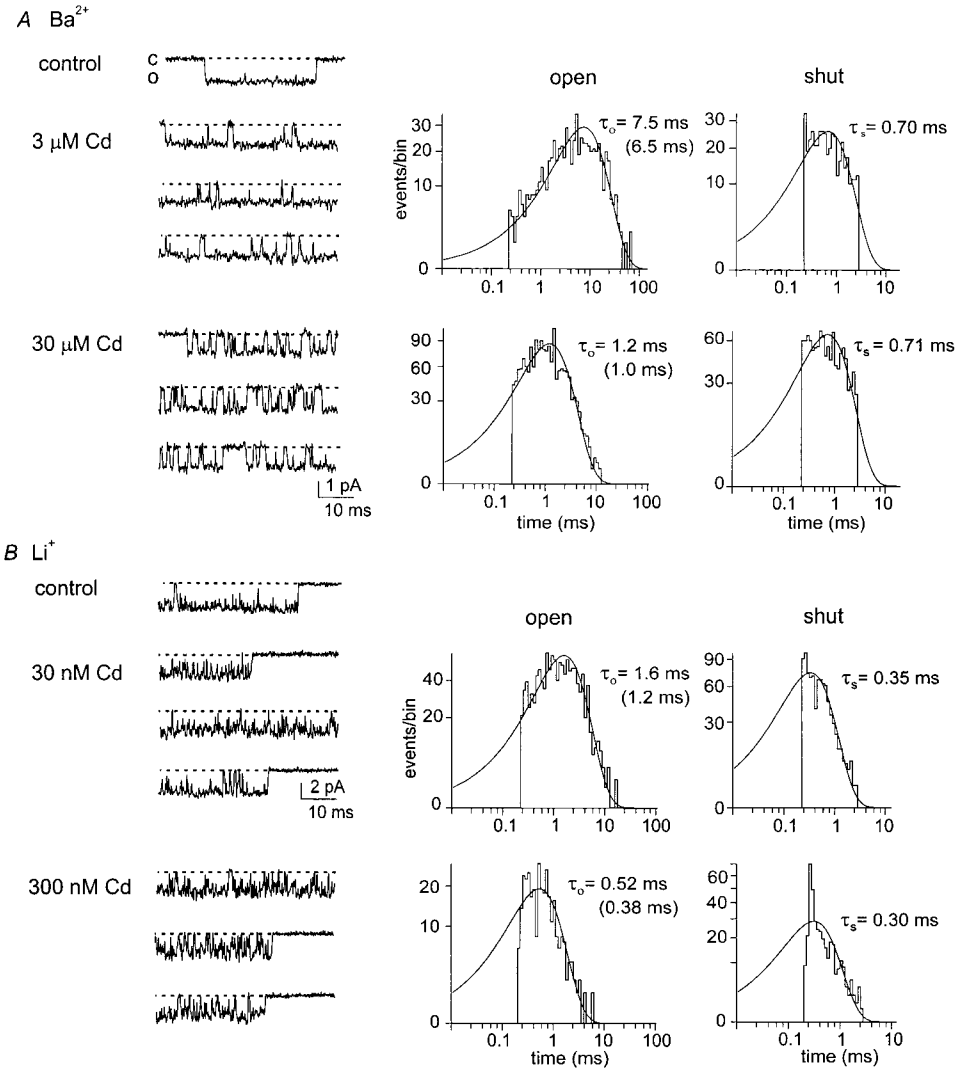

FIGURE 1. Cd^{2+} block of unitary Ba^{2+} and Li^+ currents carried by α_{1C} Ca^{2+} channels. (A) Examples of Cd^{2+} block of unitary currents carried by 110 mM Ba^{2+}, and corresponding dwell-time histograms. Test potential, 0 mV; filter corner frequency, 2 kHz; sampling rate, 10 kHz. Solid curves drawn through dwell-time histograms are the exponential fits to the binned data. Raw dwell-time constants and dwell-time constants corrected for missed events (parentheses) are indicated to the right of each histogram. (B) Examples of Cd^{2+} block of unitary currents carried by 100 mM Li^+, and fitted dwell-time histograms. Test potential, −100 mV; corner frequency, 2 kHz; sampling rate, 10 kHz. Time axis tic marks are 0.2 decades per tic.

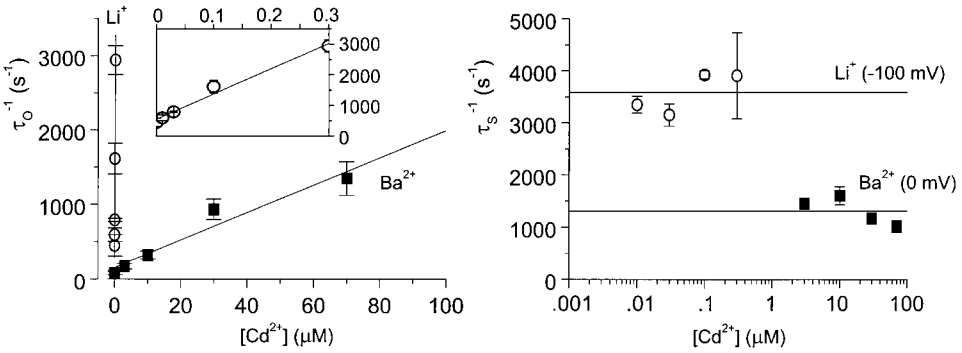

FIGURE 2. For WT channels, comparison of kinetics of Cd^{2+} block of Ba^{2+} and Li^+ currents. (Left) Plot of reciprocals of corrected open-time constants versus [Cd^{2+}] for Ba^{2+} (■; V_M = 0 mV) and for Li^+ (○; V_M = −100 mV). Linear regression fits (solid lines) to these data yield rate constants for Cd^{2+} block of Ba^{2+} (slope = 1.8×10^7 M^{-1} s^{-1}) and of Li^+ (slope = 8.2×10^9 M^{-1} s^{-1}) currents. (Inset) Cd^{2+} block of Li^+ data on an expanded scale. (Right) Plot of reciprocals of shut time constants versus [Cd^{2+}] for Ba^{2+} (■; V_M = 0 mV) and for Li^+ (○; V_M = −100 mV). Horizontal lines are drawn through the mean of all the data points and yield rate constants for Cd^{2+} block of Ba^{2+} (1,309 s^{-1}) and of Li^+ (3,538 s^{-1}) currents. For Ba^{2+} currents, n = 3–5 patches at each concentration of Cd^{2+}. For Li^+ currents, n = 3 patches at each Cd^{2+} concentration, except for 0.1 μM Cd^{2+}, for which n = 2 patches.

were also different between the Ba^{2+} and Li^+ solutions (Fig. 2, right). The τ_S^{-1} values measured for the lowest concentrations of Cd^{2+} tested probably provide the best estimate of the true off rate, but because we were unsure of the scatter in our data, we estimated off rates from the horizontal lines fitted to all of the data. Using this procedure, the Cd^{2+} off rate was 1,309 s^{-1} with Ba^{2+} as the current-carrying ion (0 mV), and 3,591 s^{-1} with Li^+ as the current-carrying ion (−100 mV). However, off rates for pore blockers such as Cd^{2+} are strongly affected by membrane potential (Lansman et al., 1986; Kuo and Hess, 1993a,b), so to compare Cd^{2+} off rates for Ba^{2+} and Li^+ currents, rates were adjusted for the −100-mV difference in potential. Based on an e-fold/−25 mV increase in off rate (Kuo and Hess, 1993a,b), the Cd^{2+} off rate at −100 mV with Ba^{2+} as the current carrier is extrapolated to 71,469 s^{-1}, ~20× faster than the Cd^{2+} off rate measured at this potential with Li^+ as the current carrier.

As a test for the reliability of the WT rate estimates, particularly for the very fast on rate of Cd^{2+} in the Li^+ solution, an independent means of estimating block and unblock rates was applied. β distribution analysis of the kinetics of Cd^{2+} block of Li^+ current yielded, for 300 nM Cd^{2+}, a block rate of 3,140 ± 1,380 s^{-1} (n = 3) and an unblock rate of 4,759 ± 1,712 s^{-1} (n = 3), as compared with threshold analysis values of 1,788 ± 128 s^{-1} (n = 3) and 3,936 ± 811 s^{-1} (n = 3), respectively. The rough similarity of the rates obtained by the two different methods of analysis provides confirmation of the results of the half-amplitude threshold analysis.

Effect of EEEE Locus Mutations on Rates of Blocker Entry and Exit: E→D Mutants

Previous work at the whole-cell level showed that EEEE locus mutations reduce pore binding affinity for divalent metal ions such as Ca^{2+} and Cd^{2+} in a mutation-specific manner (Ellinor et al., 1995). Here we have investigated the effects of EEEE locus mutations upon rates of entry and exit for a blocking ion. We have also investigated how mutation-specific block kinetics depend upon the current-carrying ion species. The substitutions studied were E→D mutants, which shortened side-chain length by one methylene carbon but pre-

TABLE II

Summary of Rate Constants and Apparent Binding Affinity for Cd^{2+} Block of Ba^{2+} and Li^{2+} Currents Carried by WT, E→D, and E→A Channels

	Ba^{2+}			Li^+		
	k_{on}	k_{off}	K'_d	k_{on}	k_{off}	K'_d
	M^{-1} s^{-1}	s^{-1}	μM	M^{-1} s^{-1}	s^{-1}	μM
WT	1.8 ± 0.26 × 10^7	1309 ± 132	73 ± 13	8.2 ± 0.64 × 10^9	3591 ± 200	0.4 ± 0.04*
E_ID	2.0 ± 0.09 × 10^7	1391 ± 85	70 ± 5	0.56 ± 0.07 × 10^9*	2003 ± 297*	3.6 ± 0.69*
E_{II}D	1.0 ± 0.07 × 10^7*	4411 ± 443*	441 ± 54*	0.76 ± 0.10 × 10^9*	3139 ± 427	4.1 ± 0.76*
E_{III}D	2.2 ± 0.12 × 10^7	8242 ± 800*	375 ± 42*	0.11 ± 0.01 × 10^9*	5541 ± 178*	50.3 ± 4.42*
E_{IV}D	2.5 ± 0.32 × 10^7	1195 ± 110	48 ± 8	0.35 ± 0.07 × 10^9*	1255 ± 243*	3.6 ± 0.98*
E_IA	2.5 ± 0.06 × 10^7*	1070 ± 151	43 ± 6	0.65 ± 0.02 × 10^9*	4034 ± 366	6.2 ± 0.60*
E_{II}A	1.4 ± 0.41 × 10^7	5509 ± 584*	393 ± 122*	0.03 ± 0.002 × 10^9*	4151 ± 267	138 ± 12.78*
E_{III}A	—	—	—	0.002 ± 0.0007 × 10^9*	4267 ± 511	2032 ± 737.96*
E_{IV}A	3.4 ± 0.12 × 10^7*	2765 ± 160*	81 ± 5	1.0 ± 0.20 × 10^9*	2263 ± 249*	2.3 ± 0.52*

Numbers of patches used to calculate means ± SEM are given in the figure legends. *Values different from WT at $P < 0.05$ (Student's t test).

served carboxylate groups, and E→A mutants, which further shortened side chain length and also eliminated one of the four carboxylate groups.

Fig. 3 shows data obtained for Cd^{2+} block of unitary Ba^{2+} currents carried by the E→D mutants. Examples of current records (Fig. 3 A), distributions of open (B) and shut (C) times, and plots of τ_O^{-1} (■) and τ_S^{-1} (○) versus [Cd^{2+}] (D) are shown. The on rates for Cd^{2+} block were little different across the four E→D mutants, and ranged from ~55% to ~140% of the on-rate value obtained for WT under these conditions (Table II). In contrast, off rates for Cd^{2+} block of Ba^{2+} current in E→D mutants were not all of the same general magnitude, and were in some cases distinctly different from WT. The Cd^{2+} off rates for $E_{II}D$ and $E_{III}D$ were significantly speeded up by the mutations (WT: 1,309 s^{-1}; $E_{II}D$: 4,411 s^{-1}; $E_{III}D$: 8,242 s^{-1}; $P < 0.01$) but those for E_ID and $E_{IV}D$ were similar to WT (E_ID: 1,391 s^{-1}; $E_{IV}D$: 1,195 s^{-1}; $P > 0.05$). The degree of increase in unbinding rate followed the order III > II > IV = I, which is almost identical to the order of the decreases in Cd^{2+} binding affinity previously reported for these mutants (III > II > I > IV) when carrying Ba^{2+} currents (Ellinor et al., 1995).

To test the reliability of the fastest estimated rate of Cd^{2+} unblock, that for $E_{III}D$, we again supplemented the half-amplitude threshold analysis with a β distribution analysis. β distribution analysis of the kinetics of Cd^{2+} block of Ba^{2+} current yielded, for 100 μM Cd^{2+}, a block rate of 2,448 ± 52 s^{-1} ($n = 3$) and an unblock rate of 5,899 ± 142 s^{-1} ($n = 3$), as compared with threshold analysis values of 2,169 ± 108 s^{-1} ($n = 3$) and 6,404 ± 261 s^{-1} ($n = 3$), respectively. Thus, the β distribution analysis confirms the results obtained from the half-amplitude threshold analysis.

Fig. 4 presents data for Cd^{2+} block of unitary Li^+ currents carried by the E→D mutant channels. The records in Fig. 4 A showed clear increases in the number of block events as [Cd^{2+}] was raised, although the size of these increases depended upon the mutation. The most obvious effects of the mutations were profound reductions in Cd^{2+} on rate (Fig. 4 D; sloped lines, ■). The $E_{III}D$ mutant (1.1×10^8 M^{-1} s^{-1}) was the most different from WT (7.5×10^9 M^{-1} s^{-1}), exhibiting a 70-fold reduction in Cd^{2+} entry rate relative to WT. Decreases in Cd^{2+} entry rate for the other E→D mutants ranged from 10- to 20-fold, with all four mutants following the order III > IV > I > II (Table II). Off rates (horizontal lines, ○) varied somewhat relative to WT, ranging from ~35% to ~155% of the WT value (Table II). For Li^+ currents, the general off-rate pattern across the E→D mutants was reminiscent of the off-rate pattern observed with Ba^{2+}, but was less pronounced (illustrated in Fig. 8 A, below).

Effect of EEEE Locus Mutations on Rates of Blocker Entry and Exit: E→A Mutants

The on and off rates obtained for Cd^{2+} block of unitary Ba^{2+} and Li^+ currents were also compared when individual glutamate residues were replaced with alanine (E→A mutants). As observed with the E→D mutants, the effect of the E→A mutations depended on the nature of the permeant ion. For the E→A mutants, examples of Cd^{2+} block of unitary Ba^{2+} current records, exponential fits to the distributions of open and shut times, and block and unblock rate plots are shown in Fig. 5. The amplitude of unitary Ba^{2+} current through the $E_{III}A$ mutant was so small at 0 mV (−0.25 pA) and Cd^{2+} unblock was so fast that block events could not be adequately resolved, and so Cd^{2+} block of Ba^{2+} current was not analyzed for this mutant. As shown in Fig. 5 C, shut-time distributions obtained for $E_{II}A$ and $E_{IV}A$ were best-fit by two exponential components in some cases, with the small, longer-duration component most likely reflecting incomplete exclusion of long closures.

For the E→A mutations, the primary effects on the kinetics of Cd^{2+} block of Ba^{2+} current were increases in the speed of Cd^{2+} exit, leaving the Cd^{2+} entry rate little changed (k_{on} increased to ~140–190% of the WT value; Table II). The Cd^{2+} exit rate was fastest for $E_{II}A$, followed by $E_{IV}A$, and both of these rates were significantly different from WT (Table II; $P < 0.01$). The rate of Cd^{2+} exit from E_IA was not significantly different from that of WT (Table II; $P > 0.01$). The fact that Cd^{2+} exit was unresolvable for $E_{III}A$ indicates that Cd^{2+} exited this mutant even more rapidly than it exited $E_{II}A$, an interpretation consistent with the fact that the $E_{III}A$ mutation was previously found to have the most severe effects on half-block values among all of the A and D mutants, and for all of the blocker/current-carrier pairs studied (Ellinor et al., 1995). The pattern of the effects of the E→A mutations on Cd^{2+} exit was similar to that of the E→D mutations, although the size of the increases in k_{off} were relatively larger for the E→A mutations (see Fig. 8 A).

With Li^+ as the current carrier, Cd^{2+} on rates were profoundly altered by E→A mutations and off rates were much less affected. $E_{III}A$ was the most severe mutation, with an on rate more than three orders of magnitude slower than WT (2.1×10^6 M^{-1} s^{-1} compared with 8.2×10^9 M^{-1} s^{-1}) (Fig. 6). The reductions in k_{on} followed the order III > II > I > IV (Table II). In general, the E→A mutations exhibited greater reductions in k_{on} than did cognate E→D mutations.

With the exception of $E_{IV}A$, Cd^{2+} off rates with Li^+ as the current carrier were not significantly affected by the E→A mutations (Student's t test, $P > 0.05$). $E_{IV}A$, like $E_{IV}D$, had a faster Cd^{2+} exit rate than did WT (Table II).

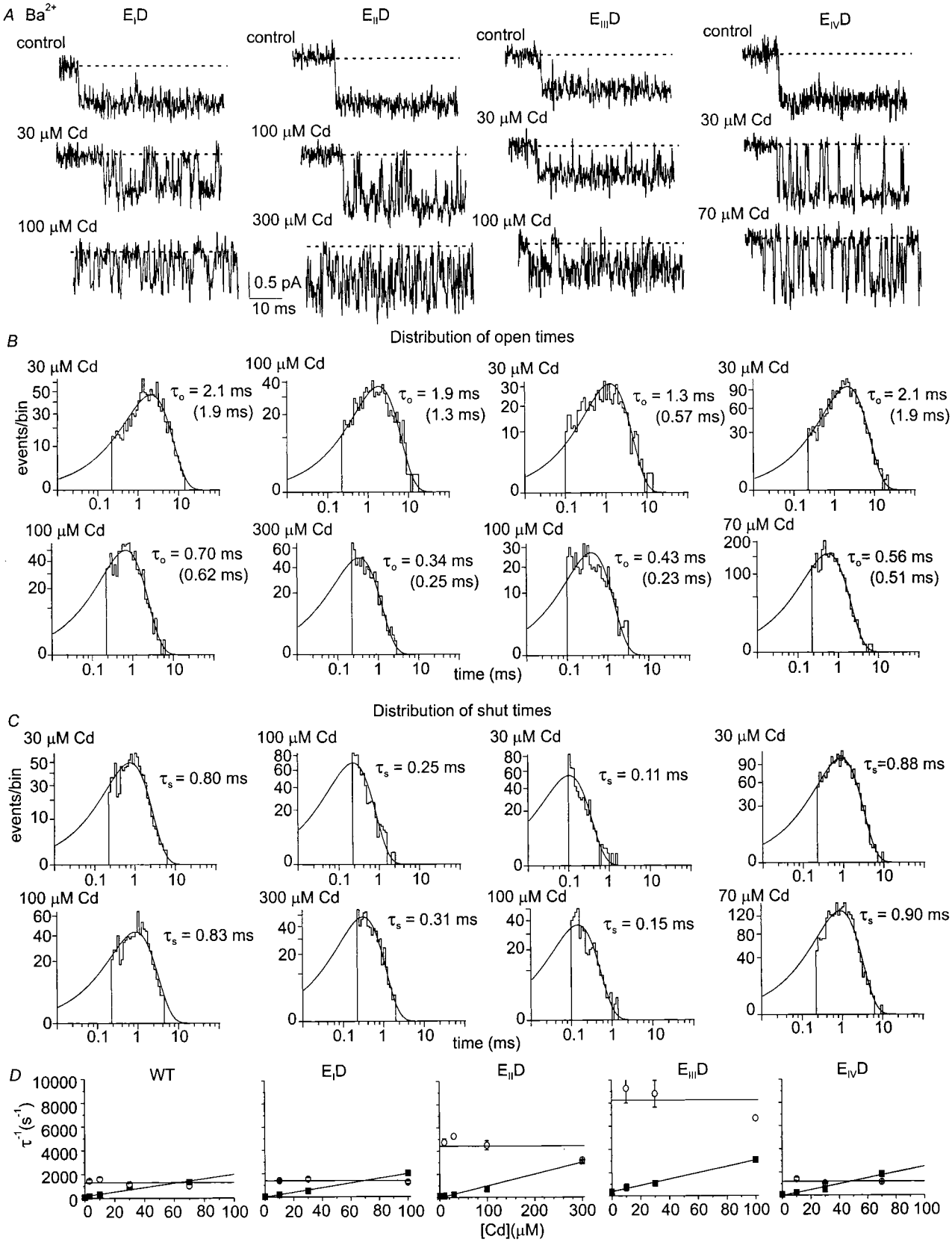
A Ba2+
EID
EIID
EIIID
EIVD
control
30 μM Cd
100 μM Cd
300 μM Cd
70 μM Cd
0.5 pA
10 ms
B
Distribution of open times
events/bin
τo = 2.1 ms (1.9 ms)
τo = 1.9 ms (1.3 ms)
τo = 1.3 ms (0.57 ms)
τo = 2.1 ms (1.9 ms)
τo = 0.70 ms (0.62 ms)
τo = 0.34 ms (0.25 ms)
τo = 0.43 ms (0.23 ms)
τo= 0.56 ms (0.51 ms)
time (ms)
C
Distribution of shut times
τs = 0.80 ms
τs = 0.25 ms
τs = 0.11 ms
τs=0.88 ms
τs = 0.83 ms
τs = 0.31 ms
τs = 0.15 ms
τs = 0.90 ms
D
WT
τ-1(s-1)
[Cd](μM)

(FIGURE 3)

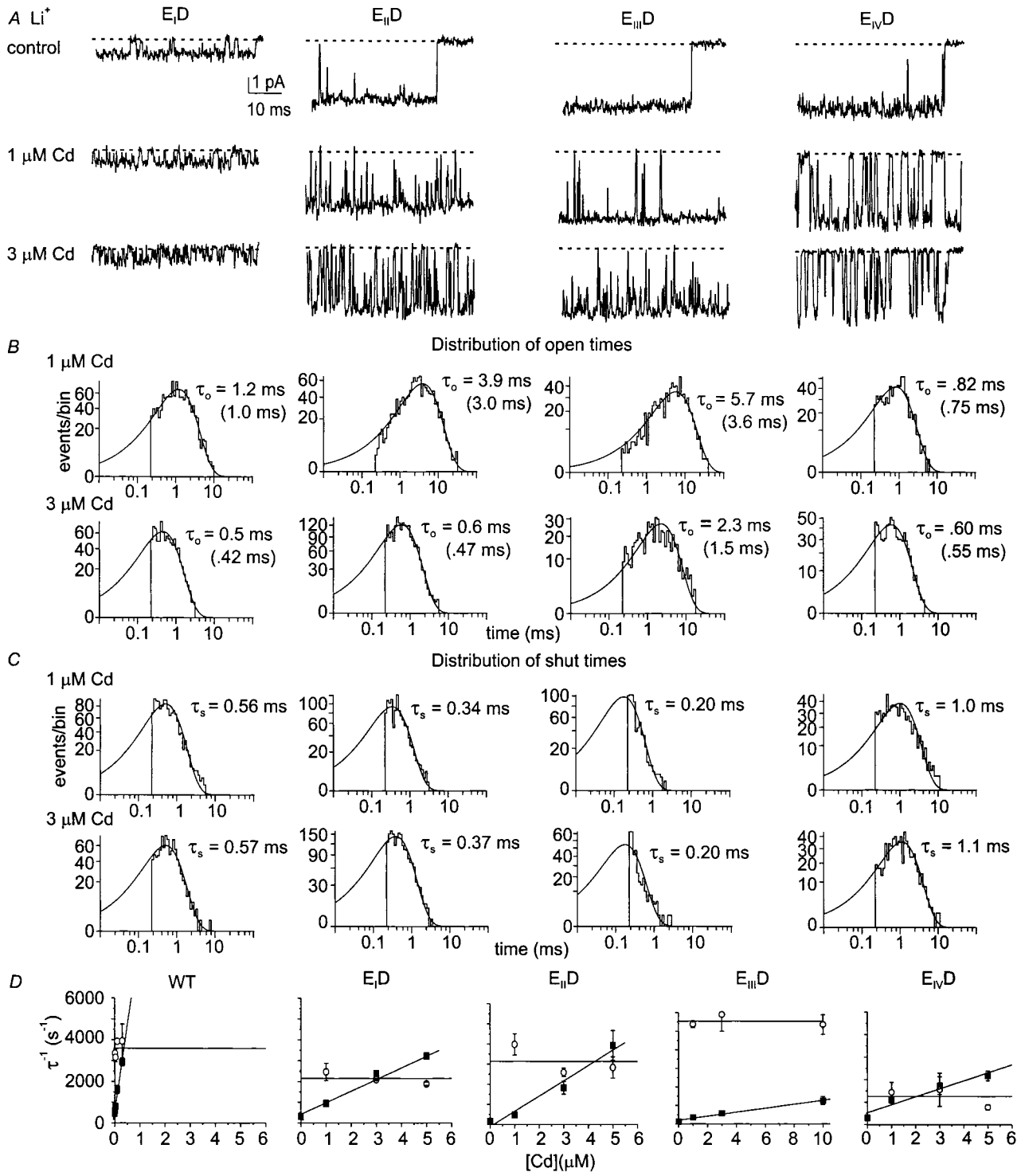

FIGURE 4. Cd^{2+} block of Li^+ current carried by single E→D mutants. (A) Single-channel records recorded at −100 mV. (B) Open-time distributions, and (C) shut-time distributions. (D) On and off rates were obtained from linear regression fits to the mean values of the shutting (■; k_{on}) and opening (○; k_{off}) rate data (n = 3–5 patches at each concentration of Cd^{2+}). Error bars not visible are smaller than the symbols.

FIGURE 3. Cd^{2+} block of Ba^{2+} current carried by single E→D mutants. (A) Single-channel records recorded at 0 mV. (B) Open-time distributions, and (C) shut-time distributions. (D) On and off rates were obtained by fitting linear regressions (solid lines) to the mean values of the shutting (■; k_{on}) and opening (○; k_{off}) rate data. At each concentration of Cd^{2+}, n = 3–5 patches, except for $E_{II}D$ at 100 μM Cd^{2+}, for which n = 2. Error bars not visible are smaller than the symbols. Time axis tic marks are 0.2 decades per tic.

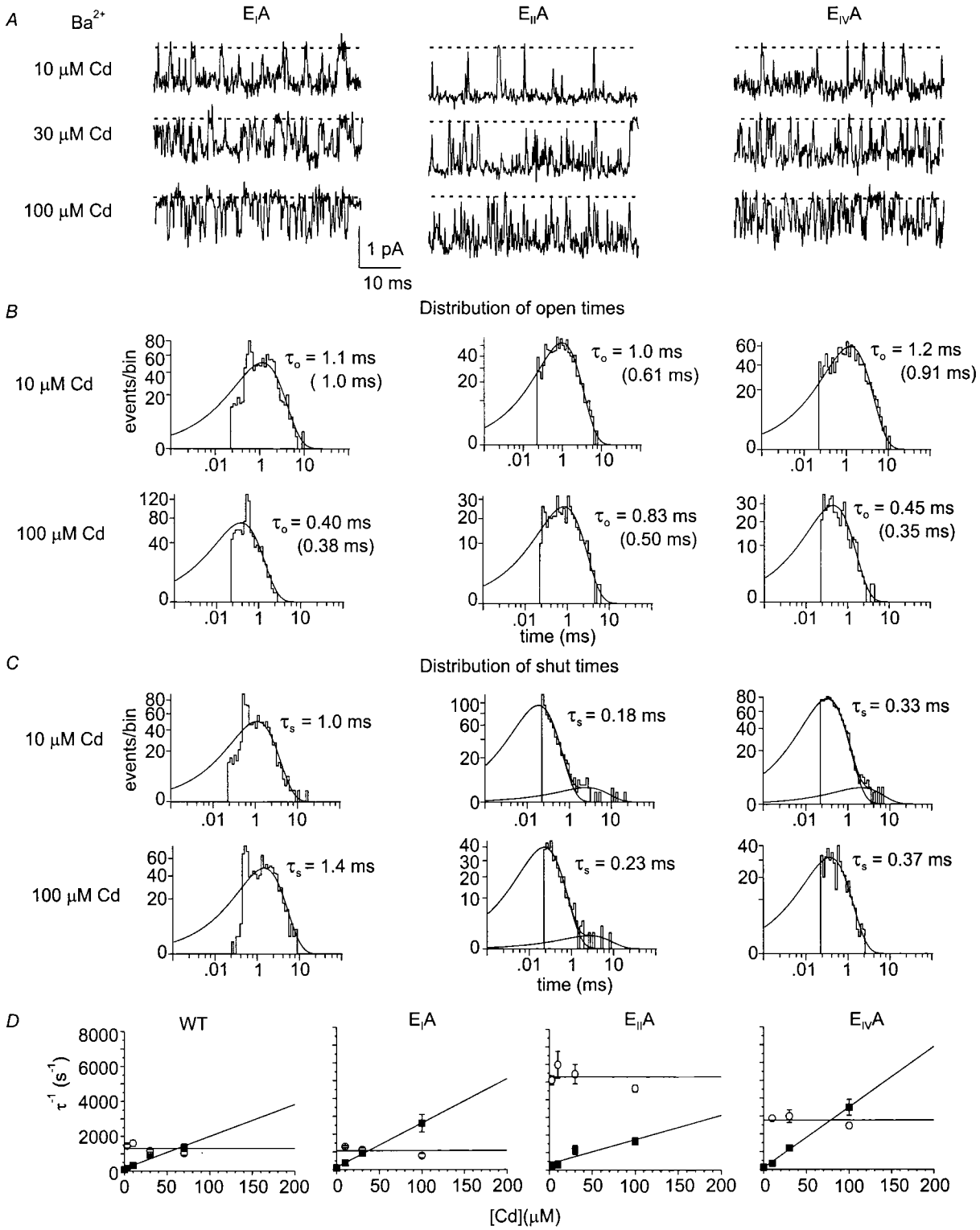

FIGURE 5. Cd^{2+} block of Ba^{2+} current carried by single E→A mutants. (A) Single-channel records at 0 mV. (B) Open-time distributions, and (C) shut-time distributions. (D) On and off rates were obtained from linear regression fits (solid lines) to the mean values of the shutting (■; k_{on}) and opening (○; k_{off}) rate data. At each concentration of Cd^{2+}, n = 3–4 patches, except for $E_{II}A$ at 0 Cd^{2+}, for which n = 2. Error bars not visible are smaller than the symbols.

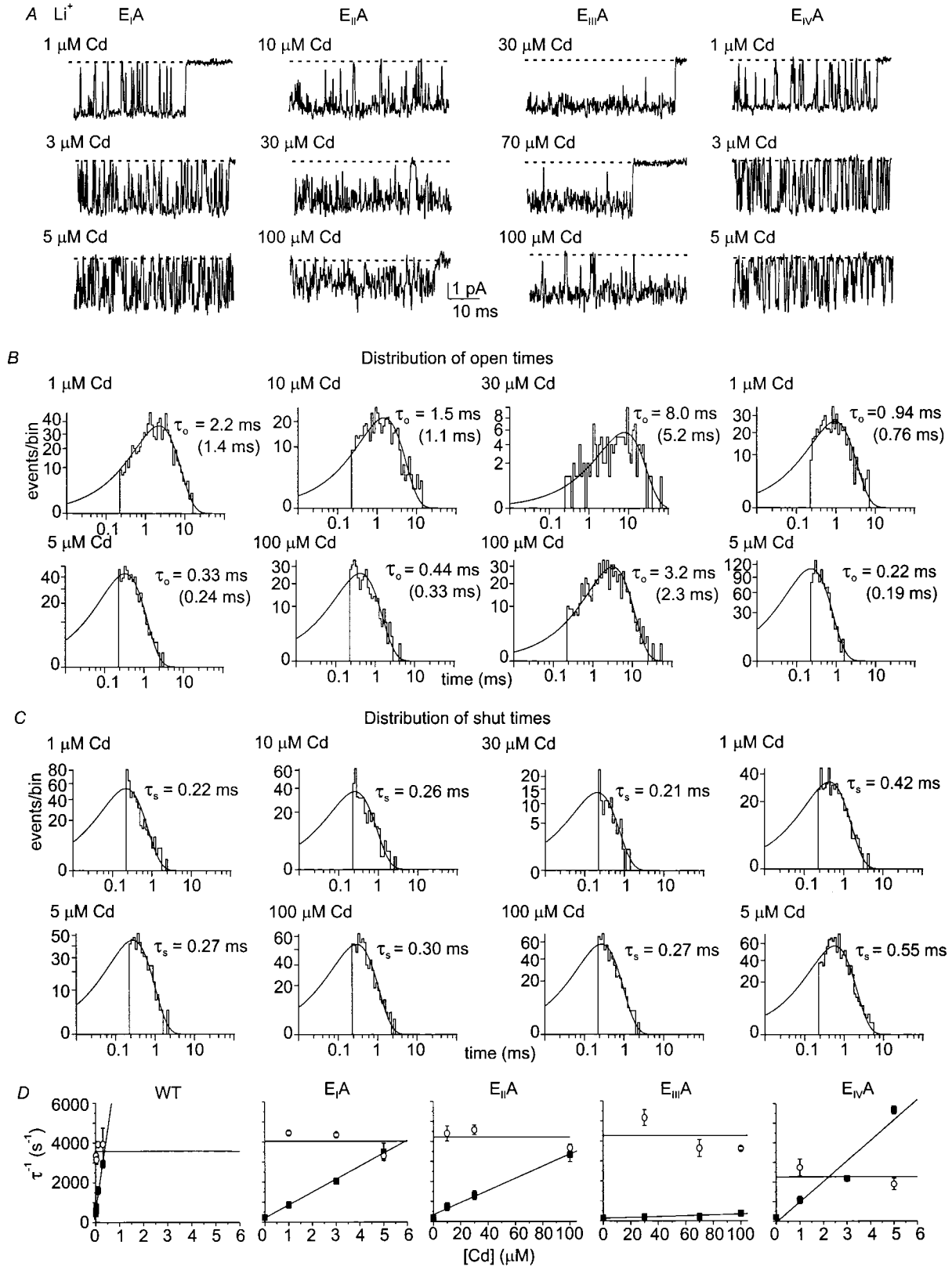

FIGURE 6. Cd^{2+} block of Li^+ current carried by single E→A mutants. (A) Single-channel records recorded at −100 mV. (B) Open-time distributions, and (C) shut-time distributions. (D) On and off rates were obtained from linear regression fits to the mean values of the shutting (■; k_{on}) and opening (○; k_{off}) rate data. At each concentration of Cd^{2+}, n = 3–7 patches, except for $E_{III}A$ at 30 μM Cd^{2+} and $E_{IV}D$ at 0 Cd^{2+}, for which n = 2 in both cases. Error bars not visible are smaller than the symbols.

Effect of the Permeant Ion Species on Entry and Exit Rates of Another Pore Blocker: Ca^{2+}

The results of the Cd^{2+} block experiments seemed to indicate that EEEE locus point mutations caused the on rate for blocker to be reduced when a monovalent cation carried the current, but when a divalent cation carried the current, these same mutations caused the off rate for the blocker to be enhanced. To examine the validity of this generalization, we studied Ca^{2+} block of Li^+ current to test whether this monovalent–divalent cation pair would exhibit behavior similar to that of Cd^{2+} block of Li^+ current. We previously analyzed Ca^{2+} block of Li^+ currents carried by the WT channel, obtaining an on rate for Ca^{2+} of 4.8×10^8 M^{-1} s^{-1} and an off rate of 3,582 s^{-1} at −60 mV (Cloues and Sather, 2000). Because comparison of these WT rates to those of severe EEEE locus mutations provided the desired test, we examined Ca^{2+} block of Li^+ current in the $E_{III}A$ channel. Discrete Ca^{2+} block events were not detectable for $E_{III}A$, perhaps because the off rate for Ca^{2+} at −60 mV was too fast in this mutant, and perhaps also because the on rate for Ca^{2+} was too slow. Either of these possibilities is consistent with the observed effects of the $E_{III}A$ mutation on Cd^{2+} block of Li^+ current (see Fig. 8). Seeking a more definitive answer, we studied the $E_{III}D$ mutant, in which discrete Ca^{2+} block events were resolved.

Fig. 7 compares Ca^{2+} block of Li^+ currents for WT and $E_{III}D$ channels. Examination of the unitary current records in A and B shows that 3 μM Ca^{2+} produced many more resolved block events in WT channels than did 100 μM Ca^{2+} in $E_{III}D$ channels. Fig. 7 C shows that the Ca^{2+} off rates were not significantly different between $E_{III}D$ and WT channels (4,748 s^{-1} versus 3,582 s^{-1}; $P > 0.1$), just as the Cd^{2+} off rates were not different between $E_{III}D$ and WT. On the other hand, the Ca^{2+} on rate for $E_{III}D$ was 55-fold slower than for WT (8.8×10^6 M^{-1} s^{-1} versus 4.8×10^8 M^{-1} s^{-1}; −60 mV), a finding consonant with the 68-fold slowing in Cd^{2+} on rate for this same mutant relative to WT (−100 mV). β distribution analysis of the kinetics of Ca^{2+} block of $E_{III}D$ yielded, for 1 mM Ca^{2+}, $k_{on} = 5{,}621 \pm 466$ s^{-1} and $k_{off} = 5{,}603 \pm 574$ s^{-1} ($n = 3$), values close to those predicted by the linear fits to the results of the threshold analysis ($k_{on} = 6{,}000$ s^{-1}, $k_{off} = 4{,}748$ s^{-1}).

DISCUSSION

In the present work on selective permeability in an L-type Ca^{2+} channel, we studied inter-ion competition for binding to the EEEE locus for ion pairs in which one ion interacted much more strongly with the EEEE locus than did the other ion. For the three pairings studied, relative WT EEEE locus affinities at 0 mV were 8.0×10^{-9} M for Cd^{2+} vs. Li^+, 7.3×10^{-5} M for Cd^{2+} vs. Ba^{2+} and 6.8×10^{-7} M for Ca^{2+} vs. Li^+. All of these ions entered the pore from the extracellular side of the channel, and all exited to the intracellular side (Lansman et al., 1986; Kuo and Hess, 1993b). A given ion acted as a blocker because its exit rate was low, or it acted as a current carrier if both its exit rate and concentration were high.

The rate of extracellular metal ion entry into the pore of an L-type Ca^{2+} channel was measured as the rate of binding of a high-affinity divalent cation (Cd^{2+} or Ca^{2+}) to the WT or mutated EEEE locus. In this single-file, multi-ion pore (Almers and McCleskey, 1984; Hess and Tsien, 1984), binding of a high-affinity cation obstructed flow of the dominant current-carrying ion (Ba^{2+}or Li^+), and the frequency of these discrete block events yielded the rate of blocking ion entry. Similarly, the rate of divalent metal cation departure from the pore and into the intracellular region was determined as the rate of unblock of unitary current. The two principal observations made in this work were (a) that the rate of metal ion entry into the pore of a WT Ca^{2+} channel depended upon the binding affinity of the ion already occupying the EEEE locus, and (b) that the way in which EEEE locus mutations reduced divalent cation binding affinity depended upon the valence of the current-carrying ion. Specifically, EEEE locus substitutions increased the permeability of Cd^{2+} when Ba^{2+} was the dominant current carrier, but the same substitutions decreased the permeability of Cd^{2+} when Li^+ was the current carrier. The interpretation of these observations is considered below.

Influence of the Current-carrying Ion on Cd^{2+} Entry into WT Channels

In the experiments on WT channels, Cd^{2+} competed with either Li^+ or Ba^{2+} for entry into the pore. Competing against Li^+, the rate of association of Cd^{2+} with the EEEE locus was 8.2×10^9 M^{-1} s^{-1}. This on rate is approximately fivefold greater than the estimated diffusion-controlled rate of association of a divalent metal ion with the EEEE locus (Kuo and Hess, 1992, 1993a), and indicates that Cd^{2+} binds to the EEEE locus at, or slightly above, the rate calculated from simple diffusional interaction. Remarkably, Cd^{2+} can apparently displace Li^+ from the EEEE locus as fast as Cd^{2+} can diffuse into the pore. The data do, however, hint at an alternative possibility that rapid Cd^{2+} displacement of Li^+ relies upon more than a diffusive process: taken at face value, the (barely) super-diffusional Cd^{2+} on rate may be a clue that divalent cations are attracted into the EEEE locus at a rate that is enhanced by electrostatic interaction with the anionic EEEE locus carboxylates (Creighton, 1993). This possibility is reminiscent of the case of proton

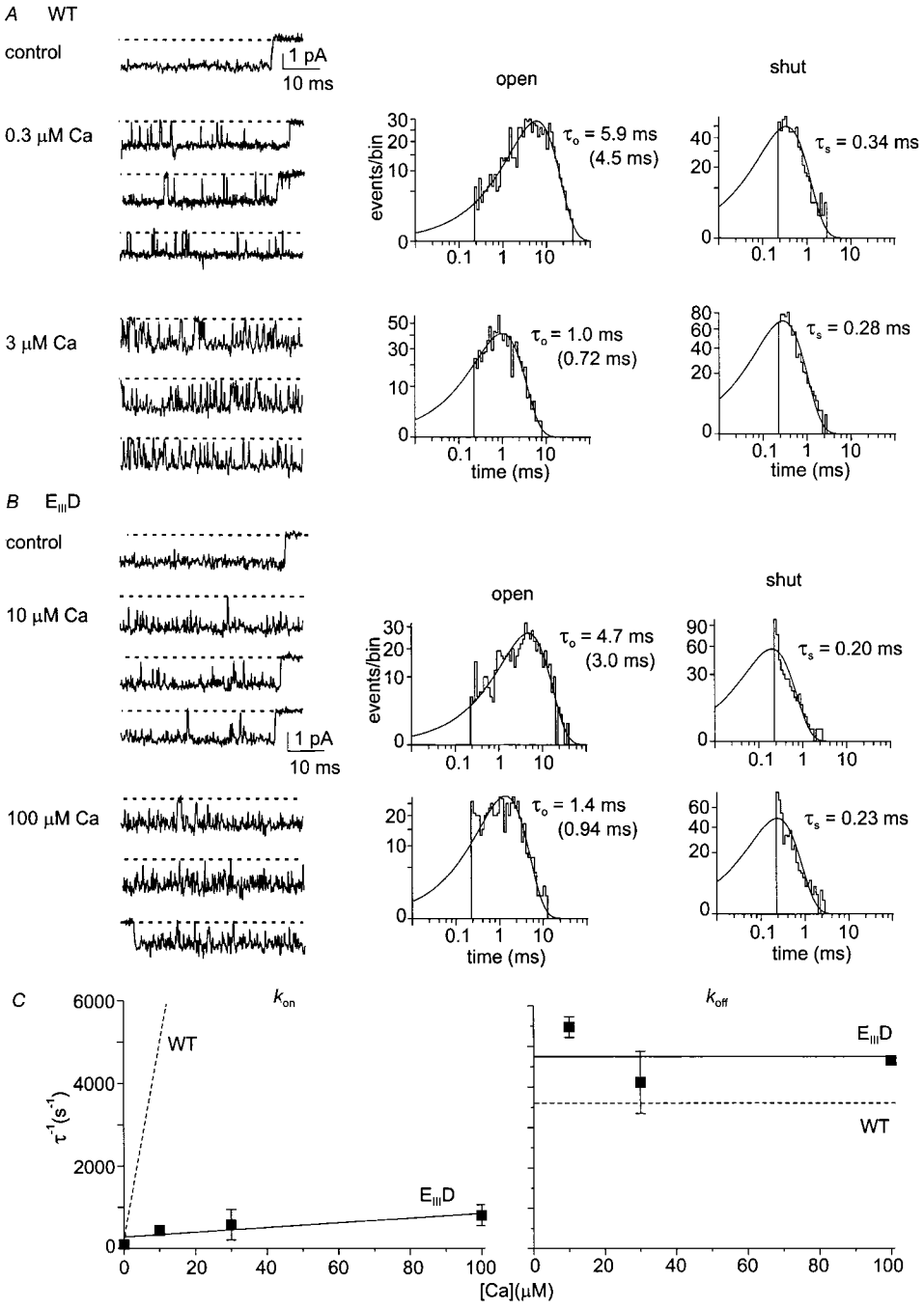

FIGURE 7. Ca^{2+} block of Li^+ current in (A) WT and (B) $E_{III}D$ channels. (C) On- and off-rate plots for Ca^{2+} block of WT and $E_{III}D$ channels. Dashed lines indicate the best fits to WT data, as previously published (Cloues and Sather, 2000). Membrane potential was −60 mV for WT and $E_{III}D$. Records were filtered at 2 kHz, and sampled at 10 kHz. At each concentration of Ca^{2+}, $n = 3$ patches. Error bars not visible are smaller than the symbols.

block of L-type Ca^{2+} channels, in which the proton association rate significantly exceeds the diffusion limit (Prod'hom et al., 1987).

Competing against Ba^{2+}, Cd^{2+} entered the pore at a rate of 1.8×10^7 M^{-1} s^{-1}, which was 1/400th the Cd^{2+} entry rate when Cd^{2+} competed against Li^+. Ba^{2+} and Li^+ differ in charge, ionic radius, water substitution rate, and enthalpy of dehydration, and any of these differences could underlie the distinctly different interactions of these ions with Cd^{2+} in the EEEE locus. One possibility is that Ba^{2+} more completely screens EEEE locus charge, so that Cd^{2+} is not as strongly attracted into a Ba^{2+}-occupied pore as it is attracted into a Li^+-occupied pore. However, it is unlikely that the effects of current-carrying ions upon Cd^{2+} on rate can be accounted for by their charge alone, because the on rate for Ca^{2+} versus Li^+ was also much lower (4.8×10^8 M^{-1} s^{-1}; Cloues and Sather, 2000) than that of Cd^{2+} versus Li^+. The most specific description of these observations is that blocker on rate in WT channels is very strongly influenced by the EEEE locus binding affinity of the current-carrying ion.

Influence of the Current-carrying Ion on Cd^{2+} Block Kinetics in EEEE Locus Mutants

In accord with previously obtained results at the whole-cell level, the severity of the effect of EEEE locus substitutions on Cd^{2+} binding affinity (K'_d), calculated from k_{off} and k_{on} (Table II), depended on the nature and location of the amino acid substitution (Ellinor et al., 1995). Substitution at residue E_{III} generally had the most profound effect, followed by substitution at E_{II}. Substitutions at residues E_I and E_{IV} had much smaller effects in general.

The pattern of substitution-specific effects upon k_{on} and k_{off} is illustrated for Ba^{2+} and Li^+ currents in Fig. 8. This summary shows that blocking ion interaction with the mutated EEEE locus depended not only on the nature and position of the amino acid substitution, but very much on the nature of the current-carrying ion as well. With Ba^{2+} as the current-carrier, D or A mutations predominantly affected k_{off} for Cd^{2+}, and had little systematic effect on k_{on}. In contrast, with Li^+ as the current-carrier, D or A mutations predominantly affected k_{on} for Cd^{2+}, with smaller effects on k_{off}. As for the k_{off}/k_{on} ratio, effects on k_{on} and k_{off} were position specific. For Cd^{2+} k_{off} values measured versus Ba^{2+}, for example (Fig. 8 A, left), k_{off} for E_ID and $E_{IV}D$ were not statistically different from the WT value ($P > 0.1$), k_{off} for $E_{II}D$ was larger than for WT ($P < 0.001$), E_ID ($P < 0.005$), and $E_{IV}D$ ($P < 0.002$), but smaller than for $E_{III}D$ ($P < 0.01$). The effects also differed between the D and A substitutions at any given position, with the A substitutions generally producing larger deviations from WT performance. Thus, the way in which the EEEE locus residues interact with a blocking ion is dependent in part upon the kinds and numbers of interactions made between the EEEE locus and other, current-carrying ions within the pore.

One way to rationalize the effects of EEEE locus mutations on block and unblock kinetics is based on consideration of the number of EEEE locus oxygen (O) atoms available to bind Cd^{2+}, Ba^{2+}, or Li^+, an approach that represents an extension of an earlier model of EEEE locus function (Yang et al., 1993). The results of investigation of proton block (Chen et al., 1996; Klockner et al., 1996) and of substituted-cysteine accessibility work (Cibulsky and Sather, 2000; Wu et al., 2000) indicate that the oxygen atoms of the EEEE locus glutamates project into the lumen of the pore, where they are presumed to interact with metal ions. In the scheme developed here, individual O atoms bind and unbind metal ions according to thermal motions in the pore and electrostatic interactions with the permeating metal ions, and metal ions attempt to bind several O atoms so that unbinding of any single O does not generally result in complete unbinding of that ion. The approximate numbers of O atoms that could interact with the metal ions is suggested by their preferred ligand coordination numbers of six for Li^+ and for Cd^{2+}, seven for Ca^{2+} and eight for Ba^{2+} (Falke et al., 1994; Martel and Hancock, 1996). We speculate that some O atom(s) must be available to bind and stabilize entering Cd^{2+}, Ba^{2+}, or Li^+ in the EEEE locus. In some trials, the

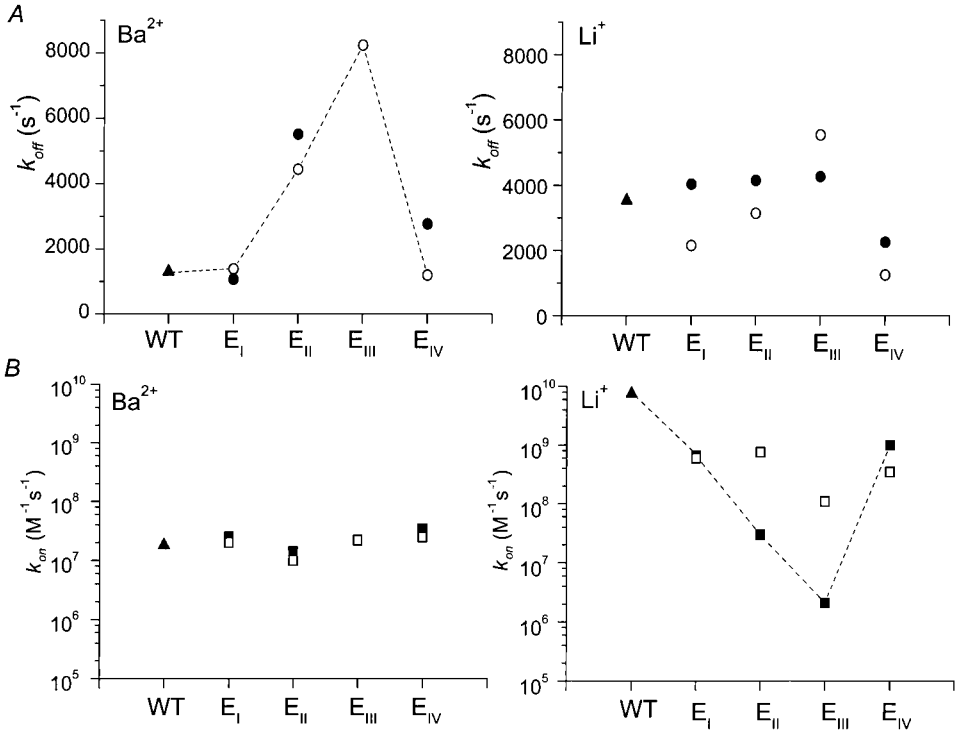

FIGURE 8. Summary of effects of individual EEEE locus mutations on the on- and off-rate constants for block by Cd^{2+}. (▲) WT values. (A) Cd^{2+} off rates for E→D (○) and E→A (●) mutants are compared for Cd^{2+} versus Ba^{2+} (left) and Cd^{2+} versus Li^+ (right). (B) Cd^{2+} on rates for E→D (□) and E→A (■) mutants are compared for Cd^{2+} versus Ba^{2+} (left) and Cd^{2+} versus Li^+ (right). Dashed lines were drawn to highlight the general effects of mutations on k_{on} and k_{off}. Note the differences in scaling on the ordinates between A and B: in A, k_{off} data are displayed on a linear scale and, in B, k_{on} data are displayed on a logarithmic scale.

entering ion fails to out compete the bound ion(s) for O atoms, and in other trials it succeeds in acquiring several O atoms. The proportion of successful entry events depends upon the relative affinities of the competing ions, so that blocking ions succeed relatively frequently when competing against lower affinity current-carrying ions, whereas current-carrying ions succeed only infrequently in displacing high-affinity blocking ions.

Blocker on rate in WT channels. Fig. 9 presents a specific depiction of this model of selectivity filter function. The depiction is intended to capture the essence of the model only, so that some of the specifics of the structure (e.g., the precise positioning of carboxylate groups) should be taken in a figurative sense. Based on earlier Ca^{2+} channel work (Kuo and Hess, 1993a,b; Yang et al., 1993; Ellinor et al., 1995; Cloues and Sather, 2000), and by analogy with other ion channels (reviewed by Khakh and Lester, 1999), the selectivity filter is envisioned as a flexible structure that changes conformation as different kinds and numbers of ions pass through it. To emphasize this idea, Fig. 9 illustrates, for Ba^{2+} versus Li^+, differing orientation angles of the glutamate side chains, differing patterns of glutamate interactions with current-carrying ions, and differing numbers of interactions made with entering Cd^{2+}.

For WT channels, the on rate for Cd^{2+} against Li^+ is higher than is its on rate against Ba^{2+} because single Li^+–O binding events are briefer in duration than are single Ba^{2+}–O events. The overall unbinding rate of Li^+ is thus faster than that of Ba^{2+}, and this allows relatively faster entry of Cd^{2+} into the EEEE locus when Li^+ is the current carrier. Turning to the difference in on rate between Cd^{2+} and Ca^{2+} that was observed when these ions were tested against Li^+, again in WT channels, the

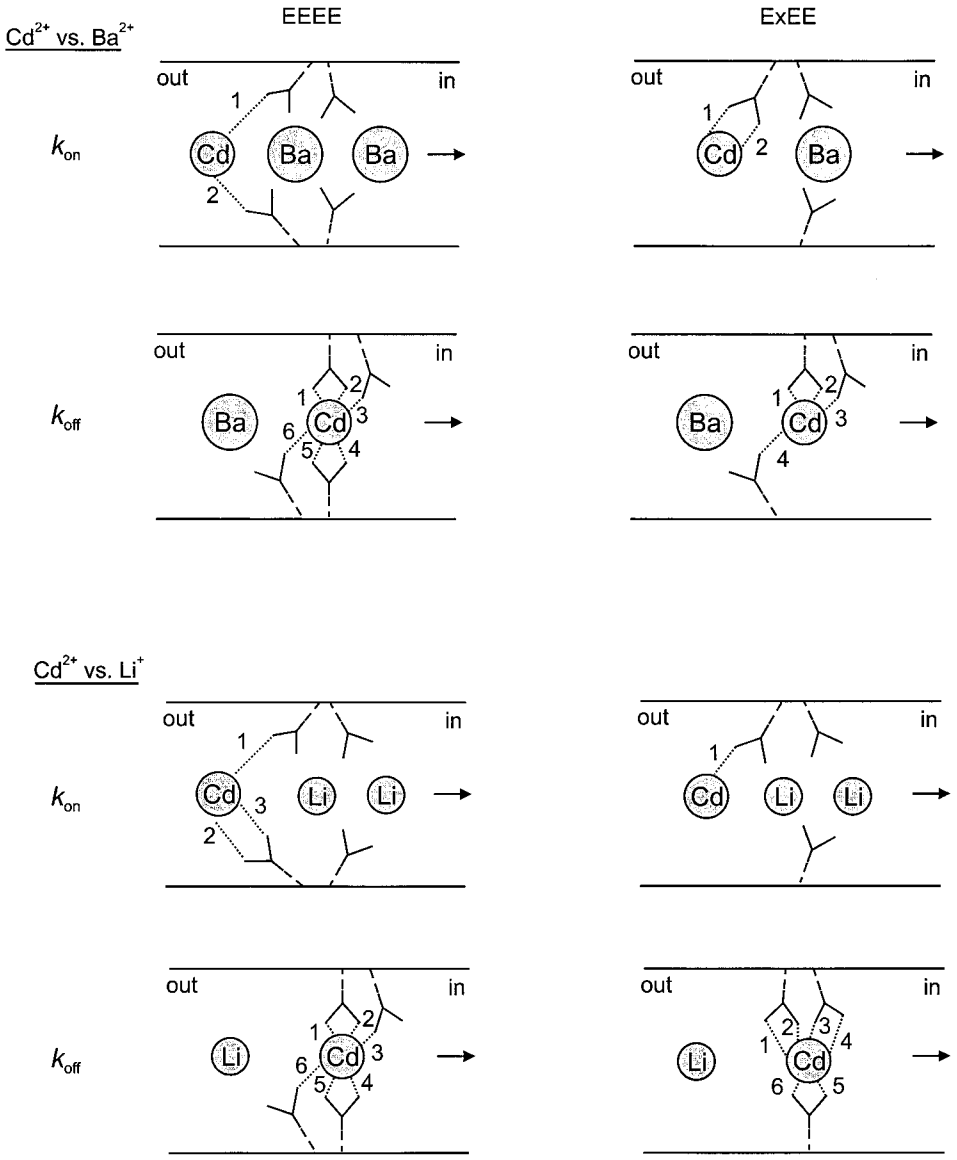

FIGURE 9. Schematic diagram illustrating a scenario that can account for the effects of permeant ion species on entry and exit rates for pore-blocking ions in WT and EEEE locus mutant channels. In the interest of clarity, numbers of oxygen atoms that might be able to interact with blocker (here indicated as Cd^{2+}) are specifically marked. Interactions with current-carrying ions are omitted. Numbers of interactions are figurative only.

comparatively slower Ca^{2+} on rate can be construed as follows: the Ca^{2+}–O binding events are briefer in duration than are the Cd^{2+}–O events, so that in competing against Li^+ for binding to EEEE locus O atoms, the probability that a Ca^{2+} ion will bind enough O atoms to displace Li^+ is lower than is the analogous probability for Cd^{2+}. The net effect is that Ca^{2+} entry into the EEEE locus is slower than is Cd^{2+} entry.

Cd^{2+} vs. Ba^{2+}: on rate. How can k_{on} for Cd^{2+} versus Ba^{2+} be essentially unaffected by EEEE locus substitutions? In cases where one of the EEEE locus residues has been replaced with D or A, there may not be enough effectively positioned O atoms remaining to properly bind two Ba^{2+} ions (Fig. 9, top row). In these cases, we propose that there is a greater probability that only one Ba^{2+} ion occupies the locus, rather than the two that more probably occupy the WT EEEE locus. With one Ba^{2+} ion in the locus of such mutants, for example E_{II} substitutions (denoted ExEE), O atoms would be available to help stabilize entering Cd^{2+}. This reasoning predicts that k_{on} for Cd^{2+} block of Ba^{2+} flux would be similar between the EEEE channel and ExEE mutants, as observed.

It is interesting that the D and A mutants are very similar to one another in having little impact on k_{on} despite the fact that the A mutants possess two fewer O atoms in the selectivity locus. This suggests that the number of O atoms is not the only critical factor, but rather that the number of O atoms in the proper spatial arrangement is important.

Cd^{2+} vs. Ba^{2+}: off rate. Pursuing the question of mutational effects on block kinetics further, how might substitution in the EEEE locus shorten the bound lifetime of a blocking ion? This could be accounted for based on the idea that Cd^{2+} unbinding involves facilitation of departure by competition with another ion in the EEEE locus (knock-off; Neyton and Miller, 1988a,b; Kuo and Hess, 1993a,b), and by making in addition the assumption that, analogous to the case for Cd^{2+} entry into a Ba^{2+}-occupied locus, Ba^{2+} can enter the Cd^{2+}-loaded mutant locus as readily as it can enter the Cd^{2+}-loaded WT EEEE locus (Fig. 9, second row). Compared with the case for WT, Cd^{2+} is not as strongly stabilized in the substitution mutants and so its Ba^{2+}-enhanced off rate is greater in the mutants than in WT.

In examining Fig. 8 A (left), two lesser points emerge. First, there is almost no effect of E_I and E_{IV} mutants on Cd^{2+} k_{off}, indicating either that the loss of O atoms normally present at these positions does not much destabilize Cd^{2+} binding or that any reduction in Cd^{2+} binding affinity is compensated by a reduced Ba^{2+} binding affinity. Second, the effects of the A mutants appear to be slightly larger than those of the D mutants, as anticipated from the fact that A substitution results in loss of two carboxylate O atoms, whereas D substitution preserves carboxylate O atoms but alters the position of two of them.

Cd^{2+} vs. Li^+: on-rate. How might the effects of mutations on block kinetics be so fundamentally different when Cd^{2+} must compete with Li^+ rather than Ba^{2+}? Consider first Cd^{2+} on rates, which are much more strongly affected by EEEE locus substitutions when Li^+, rather than Ba^{2+}, is the current carrier (Fig. 9, third row). We speculate that the mutant locus, like the WT EEEE locus, is frequently doubly occupied by Li^+ ions, because unlike the case for divalent Ba^{2+} ions, we suppose that there are sufficient O atoms to bind two monovalent Li^+ ions even in the mutant channels. However, compared with WT channels, Li^+-occupied mutant channels may lack the O atoms needed to stabilize Cd^{2+} as it attempts to enter the pore. Without this stabilization, Cd^{2+} returns to the external solution at such a high rate that the ultra-brief block events are not resolved in our recordings, k_{on} is slowed.

Cd^{2+} vs. Li^+: off-rate. Lastly, Cd^{2+} off rates measured with Li^+ currents were much less affected by mutations than were on rates, and the off-rate changes introduced by mutations were somewhat smaller for Li^+ currents than for Ba^{2+} currents. To account for the near absence of effect of mutations on k_{off} with Li^+ currents, suppose that in the mutants there remain sufficient O atoms available to bind Cd^{2+} tightly, as depicted in Fig. 9 (bottom row). In contrast to the case for Ba^{2+}, Li^+ is proposed to have such a comparatively low affinity for the EEEE locus O atoms that it is does not strongly compete against Cd^{2+} in the mutants, and hence Cd^{2+} does not experience much change in its complement of liganding O atoms. The result for the mutants is that, as for WT, Li^+ only weakly facilitates Cd^{2+} exit, and thus the rate of Cd^{2+} exit to the cytosol is little affected by the mutations.

Cd^{2+} Block Kinetics and Unitary Conductance

Is conduction of current-carrying ions (Ba^{2+} or Li^+) related in any simple way to the on and off rates of a blocking ion (Cd^{2+})? Fig. 10 shows that in this case it is not: for a narrow range in Cd^{2+} on rate, unitary Ba^{2+} flux did not vary in any systematic way over an eightfold range in Cd^{2+} off rate, nor did unitary Li^+ flux vary systematically over a 4.5-fold range in Cd^{2+} off rate and 3,600-fold range in Cd^{2+} on rate. The absence of a simple pattern in Fig. 10 indicates that the interactions between selectivity filter O atoms and current-carrying ions that occur during ion conduction must be different from those that occur between selectivity filter O atoms, current-carrying ions, and a blocking ion. In contrast to this conclusion for EEEE locus substitution mutants, we have previously found for subconductance states of the WT channel that the amplitudes of unitary Ca^{2+} currents carried by the various substates could be

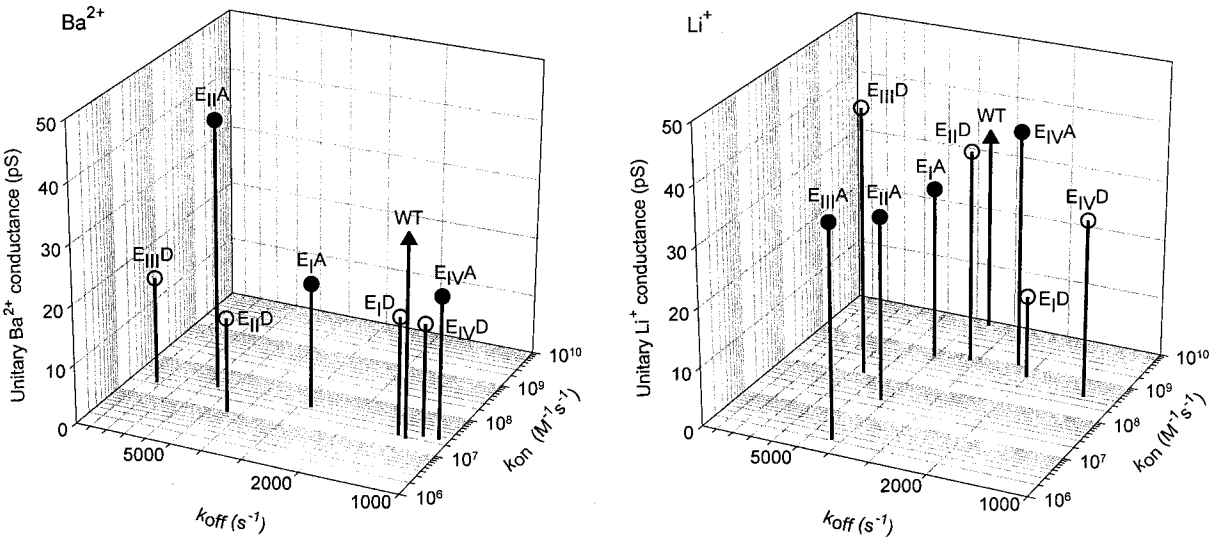

FIGURE 10. Relationships between unitary conductance and rates of Cd^{2+} block and unblock.

predicted from substate-specific on and off rates for Ca^{2+} block of Li^+ current (Cloues and Sather, 2000). These divergent conclusions might be reconciled by noting that the structure of the EEEE locus was significantly altered in the D and A substitution mutants, whereas for the WT subconductance states, EEEE locus glutamates were preserved.

The present work therefore provides a description of the way in which EEEE locus substitutions modify the flux of blocking ions, but not the flux of lower affinity, current-carrying ions. Competing against Li^+, Cd^{2+} flux was reduced in EEEE locus mutants because k_{on} for Cd^{2+} was reduced; competing against Ba^{2+} in the same mutants, Cd^{2+} flux was increased because k_{off} for Cd^{2+} was increased. Development of a more quantitative and complete model describing flux, binding, and block in the EEEE locus of Ca^{2+} channels awaits the combination of atomic-scale structure information and additional kinetic measurements.

We thank Emily Liman for the gift of a vector bearing the 5′- and 3′-untranslated regions from the *Xenopus* β globin gene, and Tsutomu Tanabe, Veit Flockerzi, and Franz Hofmann for gifts of the α_{1C}, $\alpha_2\delta_{1a}$, and β_{2b} subunit cDNAs. We thank Xin-Sheng Wu for participation in some of the experiments, and Joyce Rohan and David J. Gross for help with β-distribution analysis. Software used to simulate single channel kinetics was generously provided by Feng Qin, Anthony Auerbach, and Fred Sachs (SIMU).

This work was supported by a fellowship from the American Heart Association of Colorado and Wyoming CWFW-14-97 (R.K. Cloues), a National Research Service Award from the National Institutes of Health (NIH) MH11717 (S.M. Cibulsky), and NIH grants NS35245 and AG04418 (W.A. Sather).

Submitted: 8 May 2000
Revised: 31 August 2000
Accepted: 1 September 2000

REFERENCES

Almers, W., and E.W. McCleskey. 1984. Non-selective conductance in calcium channels of frog muscle: calcium selectivity in a single-file pore. *J. Physiol.* 353:585–608.

Armstrong, C.M., and S.R. Taylor. 1980. Interaction of barium ions with potassium channels in squid giant axons. *Biophys. J.* 30:473–488.

Armstrong, C.M., and C. Miller. 1990. Do voltage-dependent K^+ channels require Ca^{2+}? A critical test employing a heterologous expression system. *Proc. Natl. Acad. Sci. USA.* 87:7579–7582.

Armstrong, C.M., and J. Neyton. 1991. Ion permeation through calcium channels: a one-site model. *Ann. NY Acad. Sci.* 635:18–25.

Bezanilla, F., and C.M. Armstrong. 1972. Negative conductance caused by entry of sodium and cesium ions into the potassium channels of squid axons. *J. Gen. Physiol.* 60:588–608.

Chen, X.H., I. Bezprozvanny, and R.W. Tsien. 1996. Molecular basis of proton block of L-type Ca^{2+} channels. *J. Gen. Physiol.* 108:363–374.

Cibulsky, S.M., and W.A. Sather. 2000. The EEEE locus is the sole high-affinity Ca^{2+} binding structure in the pore of a voltage-gated Ca^{2+} channel: block by Ca^{2+} entering from the intracellular pore entrance. *J. Gen. Physiol.* 116:349–362.

Cloues, R.K., and W.A. Sather. 2000. Permeant ion binding affinity in subconductance states of an L-type Ca^{2+} channel expressed in *Xenopus laevis* oocytes. *J. Physiol.* 524:19–36.

Colquhoun, D., and A.G. Hawkes. 1995. The principles of the stochastic interpretation of ion-channel mechanisms. *In* Single-Channel Recording. B. Sakmann and E. Neher, editors. Plenum Publishing Corp., New York, NY. 397–482.

Creighton, T.E. 1993. Proteins: Structures and Molecular Properties. J.P. Fockler, Jr., editor. W.H. Freeman & Co., New York, NY. 253 pp.

Dang, T.X., and E.W. McCleskey. 1998. Ion channel selectivity through stepwise changes in binding affinity. *J. Gen. Physiol.* 111: 185–193.

Doyle, D.A., J.M. Cabral, R.A. Pfuetzner, A. Kuo, J.M. Gulbis, S.L. Cohen, B.T. Chait, and R. MacKinnon. 1998. The structure of the potassium channel: molecular basis of K^+ conduction and selectivity. *Science.* 280:69–77.

Ellinor, P.T., J. Yang, W.A. Sather, J.F. Zhang, and R.W. Tsien. 1995. Ca^{2+} channel selectivity at a single locus for high-affinity Ca^{2+} in-

teractions. *Neuron.* 15:1121–1132.

Ertel, E.A., K.P. Campbell, M.M. Harpold, F. Hofmann, Y. Mori, E. Perez-Reyes, A. Schwartz, T.P. Snutch, T. Tanabe, L. Birnbaumer, R.W. Tsien, and W.A. Catterall. 2000. Nomenclature of voltage-gated calcium channels. *Neuron.* 25:533–535.

Falke, J.J., S.K. Drake, A.L. Hazard, and O.B. Peerson. 1994. Molecular tuning of ion binding to calcium signaling proteins. *Q. Rev. Biophys.* 27:219–290.

Hamill, O.P., A. Marty, E. Neher, B. Sakmann, and F.J. Sigworth. 1981. Improved patch-clamp techniques for high-resolution current recording from cells and cell-free membrane patches. *Pflügers Arch.* 391:85–100.

Hess, P., J.B. Lansman, and R.W. Tsien. 1986. Calcium channel selectivity for divalent and monovalent cations. *J. Gen. Physiol.* 88: 293–319.

Hess, P., and R.W. Tsien. 1984. Mechanism of ion permeation through calcium channels. *Nature.* 309:453–456.

Hille, B. 1973. Potassium channels in myelinated nerve. Selective permeability to small cations. *J. Gen. Physiol.* 61:669–686.

Hille, B., and W. Schwarz. 1978. Potassium channels as multi-ion single-file pores. *J. Gen. Physiol.* 72:409–442.

Hille, B. 1992. Ionic Channels of Excitable Membranes. 2nd ed. Sinauer Associates, Inc., Sunderland, MA. 607 pp.

Hodgkin, A.L., and R.D. Keynes. 1955. The potassium permeability of a giant nerve fibre. *J. Physiol.* 128:61–88.

Khakh, B.S., and H.A. Lester. 1999. Dynamic selectivity filters of in ion channels. *Neuron.* 23:653–658.

Kim, M.S., T. Morii, L.X. Sun, K. Imoto, and Y. Mori. 1993. Structural determinants of ion selectivity in brain calcium channel. *FEBS Lett.* 318:145–148.

Klockner, U., G. Mikala, A. Schwartz, and G. Varadi. 1996. Molecular studies of the asymmetric pore structure of the human cardiac voltage-dependent Ca^{2+} channel. Conserved residue, Glu-1086, regulates proton-dependent ion permeation. *J. Biol. Chem.* 271:22293–22296.

Korn, S.J., and S.R. Ikeda. 1995. Permeation selectivity by competition in a delayed rectifier potassium channel. *Science.* 269:410–412.

Kuo, C.C., and P. Hess. 1992. A functional view of the entrances of L-type Ca^{2+} channels: estimates of the size and surface potential at the pore mouths. *Neuron.* 9:515–526.

Kuo, C.C., and P. Hess. 1993a. Ion permeation through the L-type Ca^{2+} channel in rat phaeochromocytoma cells: two sets of ion binding sites in the pore. *J. Physiol.* 466:629–655.

Kuo, C.C., and P. Hess. 1993b. Characterization of the high-affinity Ca^{2+} binding sites in the L-type Ca^{2+} channel pore in rat phaeochromocytoma cells. *J. Physiol.* 466:657–682.

Lansman, J.B., P. Hess, and R.W. Tsien. 1986. Blockade of current through single calcium channels by Cd^{2+}, Mg^{2+}, and Ca^{2+}. *J. Gen. Physiol.* 88:321–347.

Liman, E.R., J. Tytgat, and P. Hess. 1992. Subunit stoichiometry of a mammalian K^+ channel determined by construction of multimeric cDNAs. *Neuron.* 9:861–871.

Martel, A.E., and R.D. Hancock. 1996. Metal Complexes in Aqueous Solutions. Plenum Publishing Corp., New York, NY.

McCleskey, E.W. 1999. Calcium channel permeation: a field in flux. *J. Gen. Physiol.* 113:765–772.

McCleskey, E.W., and W. Almers. 1985. The Ca channel in skeletal muscle is a large pore. *Proc. Natl. Acad. Sci. USA.* 82:7149–7153.

Mikala, G., A. Bahinski, A. Yatani, S. Tang, and A. Schwartz. 1993. Differential contribution by conserved glutamate residues to an ion-selectivity site in the L-type Ca^{2+} channel pore. *FEBS Lett.* 335:265–269.

Mikami, A., K. Imoto, T. Tanabe, T. Niidome, Y. Mori, H. Takeshima, S. Narumiya, and S. Numa. 1989. Primary structure and functional expression of the cardiac dihydropyridine-sensitive calcium channel. *Nature.* 340:230–233.

Miller, C. 1999. Ionic hopping defended. *J. Gen. Physiol.* 113:783–787.

Moss, G.W.J., and E. Moczydlowski. 1996. Rectifying conductance substates in a large conductance Ca^{2+}-activated K^+ channel: evidence for a fluctuating barrier mechanism. *J. Gen. Physiol.* 107: 47–68.

Neyton, J., and C. Miller. 1988a. Potassium blocks barium permeation through a calcium-activated potassium channel. *J. Gen. Physiol.* 92:549–567.

Neyton, J., and C. Miller. 1988b. Discrete Ba^{2+} block as a probe of ion occupancy and pore structure in the high-conductance Ca^{2+}-activated K^+ channel. *J. Gen. Physiol.* 92:569–586.

Nonner, W., D.P. Chen, and B. Eisenberg. 1999. Progress and prospects in permeation. *J. Gen. Physiol.* 113:773–782.

Nonner, W., and B. Eisenberg. 1998. Ion permeation and glutamate residues linked by Poisson-Nernst-Planck theory in L-type calcium channels. *Biophys. J.* 75:1287–1305.

Parent, L., and M. Gopalakrishnan. 1995. Glutamate substitution in repeat IV alters divalent and monovalent cation permeation in the heart Ca^{2+} channel. *Biophys. J.* 69:1801–1813.

Pietrobon, D., B. Prod'hom, and P. Hess. 1989. Interactions of protons with single open L-type calcium channels. pH dependence of proton-induced current fluctuations with Cs^+, K^+, and Na^+ as permeant ions. *J. Gen. Physiol.* 94:1–21.

Prod'hom, B., D. Pietrobon, and P. Hess. 1987. Direct measurement of proton transfer rates to a group controlling the dihydropyridine-sensitive Ca^{2+} channel. *Nature* 329:243–246.

Sather, W.A., T. Tanabe, J.F. Zhang, Y. Mori, M.E. Adams, and R.W. Tsien. 1993. Distinctive biophysical and pharmacological properties of class A (B1) calcium channel α_1 subunits. *Neuron.* 11:291–303.

Sigworth, F.J., and S.M. Sine. 1987. Data transformations for improved display and fitting of single-channel dwell time histograms. *Biophys. J.* 52:1047–1054.

Tang, S., G. Mikala, A. Bahinski, A. Yatani, G. Varadi, and A. Schwartz. 1993. Molecular localization of ion selectivity sites within the pore of a human L-type cardiac calcium channel. *J. Biol. Chem.* 268:13026–13029.

Tsien, R.W., P. Hess, E.W. McCleskey, and R.L. Rosenberg. 1987. Calcium channels: mechanisms of selectivity, permeation, and block. *Annu. Rev. Biophys. Biophys. Chem.* 16:265–290.

Williamson, A.V., and W.A. Sather. 1999. A role for non-glutamate pore residues in the ion selection and conduction behavior of voltage-gated calcium channels. *Biophys. J.* 77:2575–2589.

Wu, X., H.D. Edwards, and W.A. Sather. 2000. Side-chain orientation in the selectivity filter of a voltage-gated Ca^{2+} channel. *J. Biol. Chem.* In press.

Yang, J., P.T. Ellinor, W.A. Sather, J.F. Zhang, and R.W. Tsien. 1993. Molecular determinants of Ca^{2+} selectivity and ion permeation in L-type Ca^{2+} channels. *Nature.* 366:158–161.

Yatani, A., A. Bahinski, G. Mikala, S. Yamamoto, and A. Schwartz. 1994. Single amino acid substitutions within the ion permeation pathway alter single-channel conductance of the human L-type cardiac Ca^{2+} channel. *Circ. Res.* 75:315–323.

Yellen, G. 1984. Ionic permeation and blockade in Ca^{2+}-activated K^+ channels of bovine chromaffin cells. *J. Gen. Physiol.* 84:157–186.

Yue, D.T., and E. Marban. 1990. Permeation in the dihydropyridine-sensitive calcium channel: multi-ion occupancy but no anomalous mole-fraction effect between Ba^{2+} and Ca^{2+}. *J. Gen. Physiol.* 95:911–939.